© 2017. Published by The Company of Biologists Ltd | Journal of Cell Science (2017) 130, 551-562 doi:10.1242/jcs.194225

RESEARCH ARTICLE

A new HECT ubiquitin ligase regulating chemotaxis and development in *Dictyostelium discoideum*

Barbara Pergolizzi[1], Enrico Bracco[2] and Salvatore Bozzaro[1,*]

ABSTRACT

Cyclic AMP (cAMP) binding to G-protein-coupled receptors (GPCRs) orchestrates chemotaxis and development in *Dictyostelium.* By activating the RasC–TORC2–PKB (PKB is also known as AKT in mammals) module, cAMP regulates cell polarization during chemotaxis. TORC2 also mediates GPCR-dependent stimulation of adenylyl cyclase A (ACA), enhancing cAMP relay and developmental gene expression. Thus, mutants defective in the TORC2 Pia subunit (also known as Rictor in mammals) are impaired in chemotaxis and development. Near-saturation mutagenesis of a Pia mutant by random gene disruption led to selection of two suppressor mutants in which spontaneous chemotaxis and development were restored. PKB phosphorylation and chemotactic cell polarization were rescued, whereas Pia-dependent ACA stimulation was not restored but bypassed, leading to cAMP-dependent developmental gene expression. Knocking out the gene encoding the adenylylcyclase B (ACB) in the parental strain showed ACB to be essential for this process. The gene tagged in the suppressor mutants encodes a newly unidentified HECT ubiquitin ligase that is homologous to mammalian HERC1, but harbours a pleckstrin homology domain. Expression of the isolated wild-type HECT domain, but not a mutant HECT C5185S form, from this protein was sufficient to reconstitute the parental phenotype. The new ubiquitin ligase appears to regulate cell sensitivity to cAMP signalling and TORC2-dependent PKB phosphorylation.

KEY WORDS: TORC2, Pia, Rictor, cAMP signalling, HECT ubiquitin ligase, HERC1, *Dictyostelium*

INTRODUCTION

Dictyostelium discoideum development is characterized by chemotaxis-driven aggregation of starving cells and subsequent differentiation of multicellular aggregates into fruiting bodies (Kessin, 2001). Cyclic AMP (cAMP) plays a morphogenetic role all over development (Gerisch, 1987; Kessin, 2001; Dormann et al., 2001). During the first hours of starvation, cAMP acts as chemoattractant by binding to the serpentine receptor cAR1, and stimulating adenylyl cyclase A (ACA) through the Gα2βγ protein (van Haastert and Devreotes, 2004). ACA stimulation triggers cAMP accumulation, which acts as a second messenger to regulate gene expression. Most cAMP is, however, released extracellularly, where it serves to relay the signal to distal cells (Gerisch, 1987; Devreotes, 1989). G-protein-dependent ACA activation requires the activity of two cytosolic proteins, Crac and Pianissimo (Pia) (Insall et al., 1994; Chen et al., 1997). Pia is the ortholog of Rictor, a subunit of the target of rapamycin complex 2 (TORC2), together with the serine-threonine kinase TOR, Lst8 and Rip3 (Lee et al., 2005). TORC2 is also responsible for the phosphorylation of the PKB (also known as AKT in mammals) proteins PKBR1 and PKBA (Lee et al., 2005; Kamimura et al., 2008). The TORC2–PDKA–PKB pathway is activated at the cell leading edge, where it regulates actin recruitment, and thus cell polarization and chemotaxis (Liao et al., 2010; Kamimura and Devreotes, 2010; Kamimura et al., 2008). Homologs of these proteins also function in metazoan chemotaxis, hence the importance of *Dictyostelium* as model organism for studying the mechanisms regulating chemotaxis and development (Bozzaro, 2013; Artemenko et al., 2014).

To identify new actors involved in chemotaxis signalling pathways, we applied saturation mutagenesis to the *Dictyostelium* temperature-sensitive aggregation-null mutant HSB1 (Bozzaro et al., 1987a). In this mutant, a point mutation in the *piaA* gene results in a single aminoacid replacement (G917D) in the Pia protein. Owing to this mutation, the cells fail to activate ACA, and thus cannot produce and relay cAMP, and aggregate, at temperatures above 18°C (Pergolizzi et al., 2002).

Here, we performed mutagenesis of the HSB1 genome by random insertion of a plasmid bearing the blasticidin resistance, leading to identification of suppressor mutants that were capable of aggregating and undergoing development to fruiting bodies. In two of these mutants, the tagged gene encoded a new protein with three conserved domains: a SPRY, PH and HECT domain. The latter displays the highest homology with the HECT domain of mammalian HERC1 ubiquitin ligases, thus we name the gene *hephA* (for HERC and PH domain), and the encoded protein HectPH1. Gene knockout by homologous recombination confirmed the rescue. We further showed that *hephA* knockout in HSB1 cells restored chemotaxis, PKBR1 and PKBA phosphorylation, short-range cAMP relay, cAMP-dependent gene expression, but not Pia-dependent adenylyl cyclase activation by cAMP pulses. Thus, *hephA* suppression rescues the HSB1 phenotype, but bypasses Pia (TORC2) and adenylyl cyclase signalling. By generating a double HSB1 and *acrA*-knockout (HSB^{acrA-}) mutant, we further show that the *acrA* gene product, adenylyl cyclase B (ACB), plays an essential role in this rescue. A model is proposed whereby inactivating the HectPH1 ubiquitin ligase increases cellular sensitivity to cAMP, allowing cell development in response to very low cAMP levels, thus suggesting that HectPH1 is involved in the desensitization of cAMP signalling.

RESULTS

Selection of HSB1 mutant suppressors by REMI saturation genetics

To identify new components involved in cAMP signalling networks, we applied a genetic suppression approach to the HSB1 aggregation-

[1]Department of Clinical and Biological Sciences, University of Torino, AOU S. Luigi, Orbassano (TO) 10043, Italy. [2]Department of Oncology, University of Torino, AOU S. Luigi, Orbassano (TO) 10043, Italy.

*Author for correspondence (salvatore.bozzaro@unito.it)

S.B., 0000-0001-6323-6190

Received 22 June 2016; Accepted 4 December 2016

Journal of Cell Science (2017) 130, 551-562 doi:10.1242/jcs.194225

deficient mutant (Bozzaro et al., 1987a). The aggregation defect in HSB1 depends on inability to activate ACA and, thus, produce cAMP. Although the cells respond to exogenously applied cAMP pulses by enhanced expression of cAMP-dependent developmentally regulated genes, and they are able to chemotax toward cAMP diffusing from a microcapillary, the HSB1 cells fail to relay cAMP. Thus, the final phenotype consists of a single cell monolayer (Fig. 1). We found by serendipity that this phenotype was temperature dependent, with the mutant being able to develop at temperatures up to 17°C, but being totally blocked above 18°C. The defective phenotype depended solely on a point mutation in the gene encoding Pia, resulting in a G917D amino acid change (Pergolizzi et al., 2002).

Since HSB1 was generated chemically, the strain is suitable for saturation mutagenesis mediated by random insertion of the blasticidin resistance sequence to generate genetic suppressors of the Pia mutation phenotype. Suppressors can be easily selected, based on their ability to form developing plaques on a bacterial lawn. Approximately 30,000 independent blasticidin-resistant transformants were generated in several rounds of transfection by electroporation, plated clonally with *E. coli* B/2 on agar and visually screened for their ability to rescue the aggregation-deficient HSB1 phenotype. Four positives clones were selected, one that was blocked at mound stage, and three that developed to fruiting bodies (Fig. 1). Two clones, #9.2 and #10.2, were further characterized genotypically and phenotypically. Clones #3.3 and #1.3 are being characterized presently.

Recovery of the flanking DNA sequences in #9.2 and #10.2 shows that gene DDB_G0286931 has been hit

To identify the genes responsible for the observed phenotype, genomic DNA from both clones was digested, and the flanking regions of the inserted plasmid were recovered and sequenced. BLAST analysis displayed sequence identity with the gene DDB_G0286931, which is 16,053 bp long and encodes a 5222-amino-acid protein (Fey et al., 2009). The gene harbours two introns and three exons. Protein analysis predicts the presence of four putative functional domains: a SPRY domain (amino acids 2620–2753), PH domain (amino acids 3834–3980), CUB domain (amino acids 4427–4512) and a HECT domain at the C-terminus (amino acids 4855–5212) (Fig. S1A). The insertion sites of pUCBsrΔBam in #9.2 and #10.2 were upstream of the PH-domain-encoding sequence, very close to each other (Fig. S1A), confirming the independent origin of the clones. The HECT domain displays 57% similarity and 38% identity with the HECT domain of mammalian HERC1 E3 ubiquitin ligases (Fig. S1B). The HERC1 family includes giant proteins, which in addition to the HECT domain all contain one or more RLD domain(s), with facultative SPRY and/or other domains (Garcia-Gonzalo and Rosa, 2005). The RLD domain is missing in the *Dictyostelium* protein. On the other hand, no HERC or HECT ubiquitin ligases have been described, to our knowledge, containing a PH domain. Thus, we named the gene *hephA* and the encoded protein HectPH1, to highlight the presence of the PH and HECT domain.

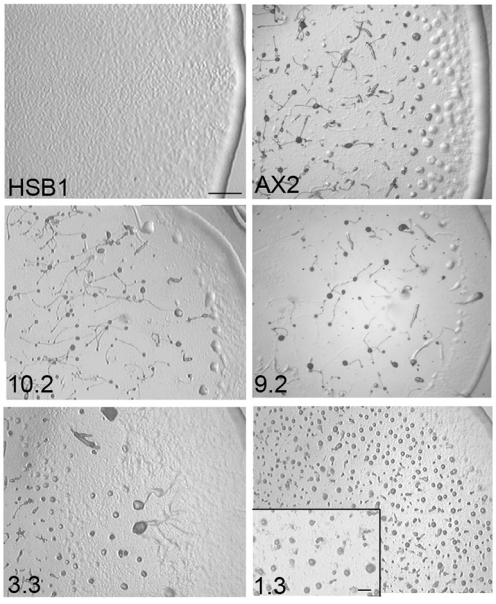

Fig. 1. Development is restored in HSB1 suppressor mutants. The four clones in which development was rescued following random gene tagging with a plasmid bearing the blasticidin resistance are shown. Resistant cells were plated with bacteria on agar plates. Fruiting bodies, slugs and, closer to the growing front, aggregates with streams are evident in clones #10.2 and #9.2, similar to the AX2 wild type. In #3.3, a larger area of non-aggregating cells is evident, with aggregates, slugs and small fruiting bodies in the middle of the plaque. In #1.3 the final phenotype consists mostly of small aggregates, and some tip mounds. The parental HSB1 strain fails to aggregate, forming a cell monolayer. Scale bars: 1 mm.

To confirm that #9.2 and #10.2 phenotype was due to REMI insertion into the DDB_G0286931 gene, a knockout strain was created by homologous recombination (Fig. S2A). Upon HSB1 transfection, colonies forming fruiting bodies on agar were obtained, and recombination in the DDB_G0286931 gene was confirmed by Southern blotting (Fig. S2B). Thus, we name the double mutant HSB1$^{HectPH1-}$. The same approach was used to generate knockout mutants in the parental AX2 strain. *HephA* disruption in AX2 led to a 3–4 h delay in tight aggregate formation, and asynchronous postaggregative development (Fig. 2). Starving cells were also plated on agar at different densities, to test to what extent aggregate formation depended on cell density. The aggregation efficiency declined to a similar extent for AX2, AX2$^{HectPH1-}$ and HSB1$^{HectPH1-}$ cells with decreasing cell density (Fig. 2B). HSB1 failed to aggregate at all densities tested, consistent with previous data (Bozzaro et al., 1987a). Thus, inactivating HectPH1 in HSB1 restores the ability of cells to spontaneously aggregate by chemotaxis, with the cells able to make short streams (see Movie 1). It is worth mentioning that HSB1 cell aggregates formed under shaking after 5 to 8 h cAMP pulsing, once deposited on glass or agar, slowly disaggregate and fail to re-aggregate and complete development (Bozzaro et al., 1987a).

We cloned the *hephA* gene fragment encoding the HECT domain, and fused it with GFP, to test whether this fragment was sufficient for rescuing the HSB1$^{HechtPH1-}$ mutant. Sequence alignment with other HECT ubiquitin ligases highlights a conserved cysteine residue that is predicted to be necessary for transferring the ubiquitin moiety to target proteins (Fig. S1B; Scheffner et al., 1995). We thus generated a mutated HECT fragment by site-directed mutagenesis, using the wild-type (wt) pDEX-HECT^{wt}-GFP vector as template to construct the vector pDEX-HECT^{C5185S}-GFP. Both vectors were transfected into the HSB1$^{HectPH1-}$ strain, and G418-resistant cells were cloned on agar plates with bacteria to assess the phenotype. Most colonies of cells transfected with pDEX-HECT^{wt}-GFP failed to form fruiting bodies, in sharp contrast to cells transfected with pDEX-HECT^{C5185S}-GFP (Fig. 3A,D). Thus, overexpressing the wild-type HECT domain of HectPH1 is sufficient to abolish the rescue of aggregation seen in HSB1$^{HectPH1-}$, with cells showing a HSB1 aggregation-less phenotype, whereas the C5185S mutation does not, suggesting impairment of the enzymatic activity.

Journal of Cell Science (2017) 130, 551-562 doi:10.1242/jcs.194225

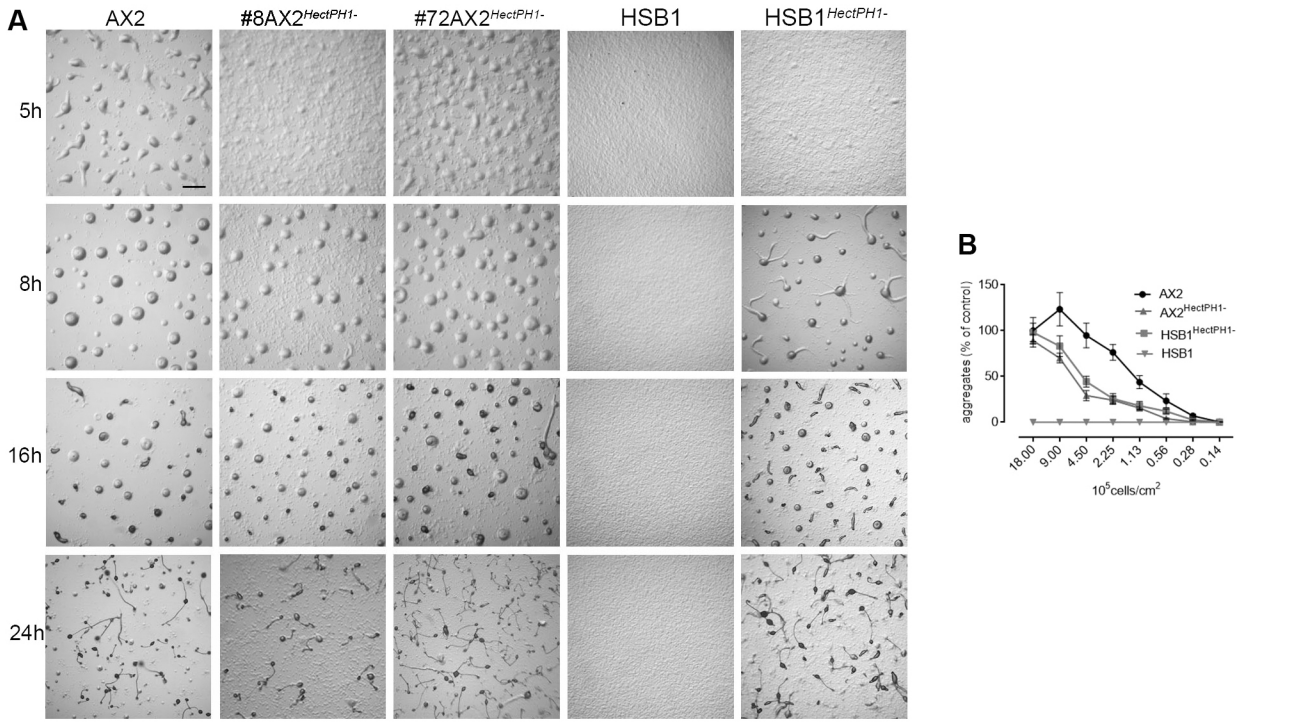

Fig. 2. Phenotypes of HectPH1-null mutants. (A) Two different AX2 HectPH1-knockout clones are shown (#8 and #72), which display a 3–4 h delay in the onset of aggregation and tight aggregate formation, whereas postaggregative development is mostly unaltered but asynchronous, as many cells fail to aggregate after 24 h. HSB1$^{HectPH1-}$ develops with timing comparable to the AX2$^{HectPH1-}$, whereas the parental HSB1 fails to aggregate. A 0.1 ml drop of starving cells at a concentration of 10^7 per ml was plated on phosphate agar and development followed over 24 h. Scale bars: 1 mm. (B) Correlation between initial cell density and efficiency to aggregate by chemotaxis. The number of aggregates, formed by each strain at the cell density indicated in the *x*-axis, was normalized to that of AX2, taking as 100% the AX2 value at the highest density (235±35 aggregates/cm^2). Aggregates of non-homogenous size account for the increase observed between 18×10^5 and 9×10^5 cells per cm^2 in AX2 cells. Starving cells were plated on agar as in A and aggregates counted after 14 h. Results are the mean±s.e.m. values of three experiments performed in duplicate (%).

Similarly, in AX2$^{HechtPH1-}$, expression of the HECT^{wt} domain, but not the HECT^{C5185S} domain, also led to cells displaying the parental AX2 phenotype (data not shown). Cells were also observed for GFP labelling, and for both plasmids a nuclear localization, confirmed by DAPI staining, was evident, although the mutant form was also found in smaller or larger clumps dispersed in the cytosol (Fig. 3B, C,E,F). Surprisingly, expression of both plasmids in the parental AX2 or HSB1 strains led only to transient fluorescence in the cell population, and selection of stable clones was unsuccessful, despite repeated attempts.

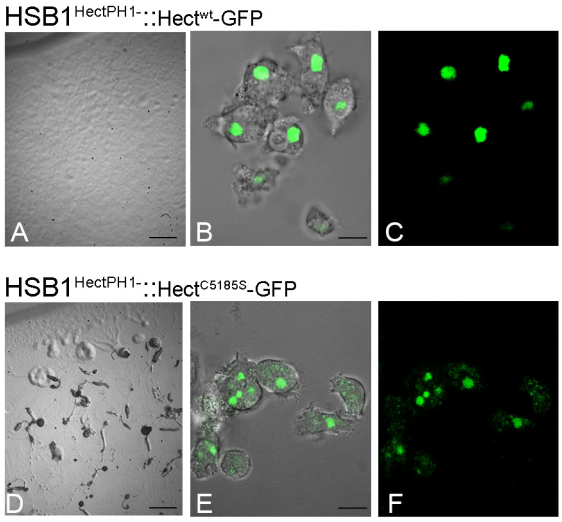

Fig. 3. Phenotype rescue of HSB1$^{HectPH1-}$ expressing HectPH1 HECT^{wt} domain. (A,D) The original HSB1 aggregation-less phenotype was restored in the HSB1$^{HectPH1-}$ suppressor mutant expressing the wild-type HECT domain (Hect^{wt}), but not with the mutated C5185S HECT, domain. Scale bars: 1 mm. (B,C,E,F) The HECT^{wt}, or HECT^{C5185S}, domain fused with GFP is recruited to the nucleus, although HECT^{C5185S} is also found in punctae and larger clumps dispersed in the cytoplasm. Scale bars: 5 µm.

Cell polarity and chemotaxis are restored in the suppressor mutant HSB1$^{HectPH1-}$

Spontaneous HSB1$^{HectPH1-}$ cell aggregation is accompanied by the ability to form streams (Movie 1), although these are shorter than in the AX2 strain. Since the HSB1$^{HectPH1-}$ mutant was able to aggregate even at low density (Fig. 2), we examined whether chemotaxis and cAMP responses were fully recovered. Upon stimulation with cAMP diffusing from a microcapillary, 5-h starved HSB1$^{HectPH1-}$ cells displayed an elongated morphology, moved smoothly towards the microcapillary and formed short streams, resembling AX2 wild-type cells (Fig. 4A; Table S1). cAMP-pulsed HSB1 cells, though responding chemotactically, failed to form streams and moved with reduced speed towards the capillary as single cells (Fig. 4A; Table S1), in agreement with their inability to relay cAMP (Pergolizzi et al., 2002).

To assess the chemotactic efficiency, HSB1$^{HectPH1-}$ and AX2$^{HectPH1-}$ cells were exposed to different cAMP gradients. At 0.1 mM cAMP diffusing from the capillary, the chemotaxis index (i.e. directionality for both mutants) was comparable to AX2, with its efficiency decreasing gradually with increasing distance from the microcapillary. At 0.01 mM cAMP, directionality had already

Journal of Cell Science (2017) 130, 551-562 doi:10.1242/jcs.194225

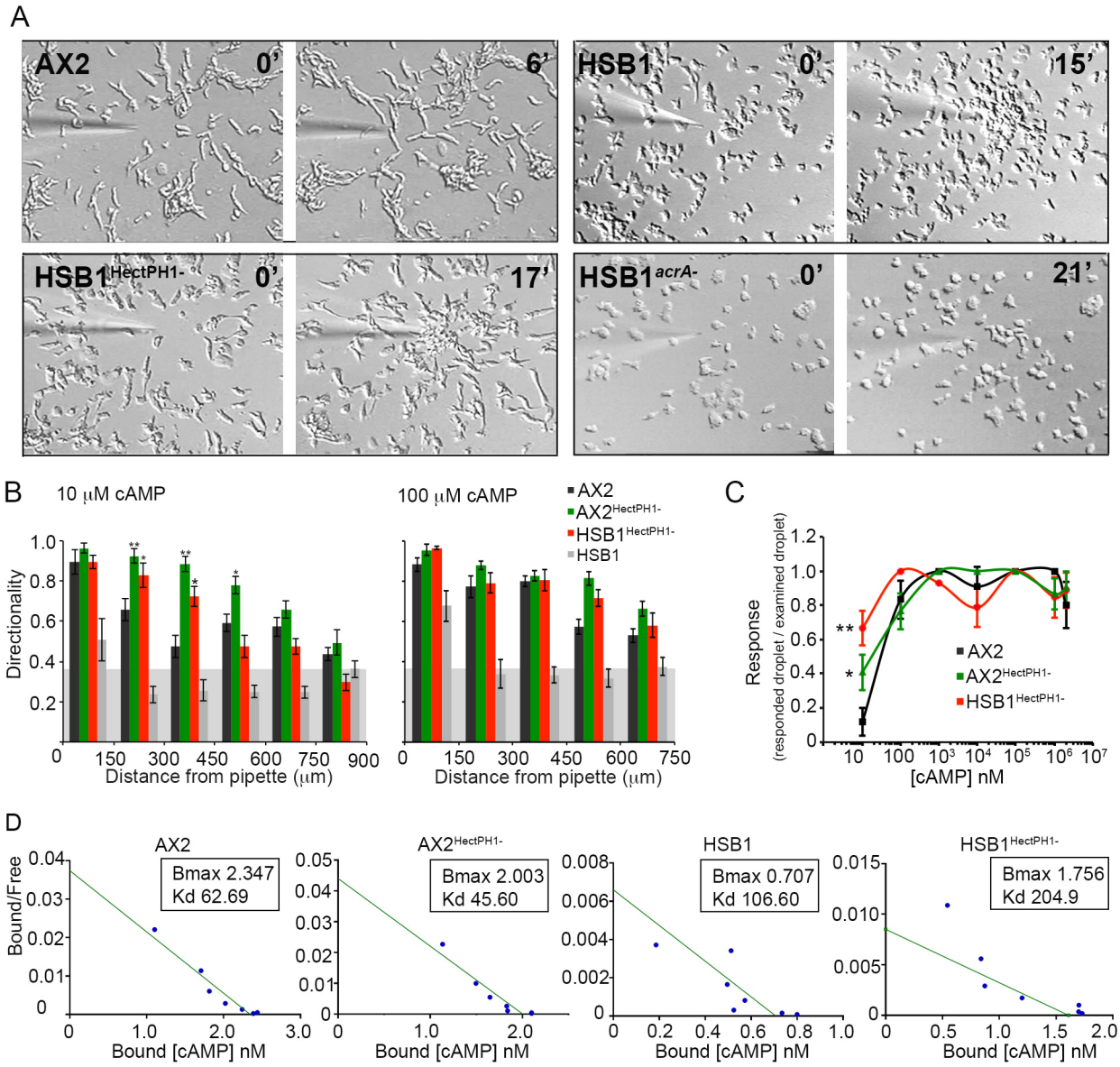

Fig. 4. Cell polarization and chemotaxis are restored in HSB1$^{HectPH1-}$ cells but totally blocked in HSB1^{acrA-} cells. (A) cAMP-pulsed HSB1 cells respond chemotactically to cAMP diffusing from a microcapillary, but the cells are only slightly polarized and move toward the capillary as single cells, failing to form streams. HSB1$^{HectPH1-}$ cells polarize and form streams, although these are shorter compared to the wild-type AX2 cells. In the cAMP-pulsed mutant HSB1^{acrA-}, in which the adenylyl cyclase B (ACB)-encoding gene *acrA* has been disrupted, cells do not polarize and move randomly. Quantitative chemotaxis parameters for each strain are shown in Table S1. Times shown (in min) are from the start of cAMP stimulation. (B) Cells were stimulated with cAMP at the concentration indicated, and chemotaxis was recorded as in A, but at lower magnification to capture cells at higher distance from the capillary. The movies were analysed for chemotactic parameters. Changes in chemotaxis index (directionality) with increasing distance are shown for each strain as the mean±s.e.m. for 10 to 35 cells for each indicated distance. *P<0.05, **P<0.005 (t-test, one-tailed) compared with AX2. (C) The small population chemotactic assay was performed at the indicated cAMP concentrations. Values are the mean±s.e.m. of four experiments with two to 10 replicates. *P<0.05, **P<0.005 (t-test, one-tailed) compared with AX2. (D) Scatchard plots of cAMP binding data. Receptor affinity was determined by the binding of [^{3}H]cAMP to cells in the presence of increasing amounts of cAMP. Maximal cAMP binding (B_{max}) is indicated for each strain. Curve fitting R^2 values for cAMP saturation binding ranged from 0.91 to 0.99. The experiment was repeated twice with a similar trend.

decreased drastically for AX2 at a distance between 150 and 450 μm, remaining constant thereafter (Fig. 4B), very likely because cells relay the cAMP signal (McCann et al., 2010). AX2$^{HectPH1-}$ and HSB1$^{HectPH1-}$ cells displayed a higher directionality, with a gradual decrease with increasing distance up to 750–900 μm, with HSB1$^{HectPH1-}$ showing random motility at this latter distance range (Fig. 4B). Indeed, HSB1 cells, which are unable to relay, displayed reduced, although chemotactically still significant, directionality at both cAMP concentrations, but a rapid decrease to values corresponding to random motility (Fig. 4B). After 5 h starvation, cells were also tested for chemotaxis in the small population assay (Kamimura et al., 2009). AX2 cells were less responsive than AX2$^{HectPH1-}$ and HSB1$^{HectPH1-}$ at concentrations below 100 nM (Fig. 4C). Taken together, these results suggest that inactivating HectPH1, both in the AX2 and HSB1 genetic background, increases cell sensitivity to cAMP signals.

To assess whether this differential sensitivity to cAMP could be due to altered cAMP receptors, cAMP-binding assays were

Journal of Cell Science (2017) 130, 551-562 doi:10.1242/jcs.194225

performed in 5-h starved cells. cAMP binding kinetics were roughly similar, with a maximal cAMP binding (B_{max}) that was comparable for all strains except HSB1, as expected, since cells were not stimulated with cAMP pulses, and thus expressed lower levels of cAR1 receptors (Pergolizzi et al., 2002). The range of dissociation constants (K_d) was comparable for AX2, HSB1 and AX2$^{HectPH1-}$, but was 2.64±0.28-fold (mean±s.e.m.) higher for HSB1$^{HectPH1-}$ (Fig. 4D). The higher dissociation constant displayed by HSB1$^{HectPH1-}$ indicates a lower affinity of membrane receptors for cAMP, which could result in increased sensitivity to cAMP (Xiao et al., 1999).

Chemotactic cell motility is regulated by a TORC2–PDKA–PKB (PKBA and PKBR1) signalling network, that transduces G-protein and RasC- or RasG-linked membrane signals to the actin cytoskeleton, leading to cell polarization and oriented movement (Lim et al., 2001; Sasaki et al., 2004; Cai et al., 2010; Zhang et al., 2008; Lee et al., 2005; Kamimura et al., 2008). PKBA and PKBR1 are transiently phosphorylated within seconds after cAMP stimulation (Meili et al., 2000; Kamimura et al., 2008; Kamimura and Devreotes, 2010). In addition PKB-dependent phosphorylated proteins, involved in cytoskeletal reorganization, have been identified (Kamimura et al., 2008). PKBR1 and PKBA activation appears to require sequential phosphorylation by TORC2 and PDKA, which phosphorylate, respectively, the hydrophobic motif (HM) and the activation loop (AL) in both proteins (Kamimura et al., 2008; Kamimura and Devreotes, 2010; Liao et al., 2010).

To assess whether this network was restored in HSB1$^{HectPH1-}$, cells were stimulated with cAMP and phosphorylation events followed with antibodies recognizing specifically the phosphorylated forms of the HM and AL of PKBR1 and PKBA, as well as their phosphorylated substrates (Kamimura et al., 2009). cAMP stimulation triggered transient phosphorylation of PKBR1, PKBA and their substrates in AX2 but not in HSB1 cells (Fig. 5A). Thus, the point mutation in HSB1 *piaA* abrogates PKBR1 and PKBA phosphorylation and their activity, as in the Pia-null mutant (Kamimura et al., 2008; Liao et al., 2010), confirming that Pia–TORC2 kinase activity is a pre-requisite for full phosphorylation of PKBR1 and PKBA. Remarkably, the phosphorylation pattern of PKBR1, PKBA and their substrates was restored in the HSB1$^{HectPH1-}$ suppressor mutant (Fig. 5A). Thus, HectPH1 deletion rescued both chemotactic cell polarity and the underlying PKB phosphorylation and kinase activity. PKBR1 and PKBA phosphorylation was also analysed in the AX2$^{HectPH1-}$ mutant. Compared to parental AX2 cells, the phosphorylation pattern followed a similar kinetics, but phosphorylation was sustained for longer in the mutant (Fig. 5B). Taken together, these results are consistent with TORC2 activity being restored in HSB1$^{HectPH1-}$, a different kinase replacing TORC2 being activated or, alternatively, a phosphatase being inhibited upon HectPH1 deletion.

G protein-linked activation of ACA is not rescued in the suppressor mutant

cAMP relay depends on GPCR-linked ACA stimulation, which requires Pia activity (Chen et al., 1997) and is defective in HSB1 (Pergolizzi et al., 2002). To test whether ACA stimulation was restored in HSB1$^{HectPH1-}$, cells were synchronized with periodic cAMP pulses for 5 h under shaking and subjected to a cAMP assay. Under these conditions, in response to a cAMP pulse, AX2 cells produce a transient burst of cAMP (Fig. 6), due to transient stimulation of adenylyl cyclase (Gerisch, 1987; Devreotes, 1989). As expected, in HSB1 cells this response was absent (Fig. 6A; Bozzaro et al., 1987a). Surprisingly, no cAMP increase was detectable in HSB1$^{HectPH1-}$ cells as well (Fig. 6A). The experiment was repeated four times between 5 and 8 h of cAMP pulsing, with a similar trend (Fig. S3A). We also measured changes in cAMP accumulation in starving cells. In AX2, cAMP accumulated more than 10-fold during starvation, whereas in both HSB1 and HSB1$^{HectPH1-}$ cAMP concentration remained at vegetative level (Fig. 6B). Thus, it appears that in HSB1$^{HectPH1-}$, G protein- and Pia-dependent ACA stimulation is not restored.

cAMP-dependent developmental gene expression and PKA activity in HSB1$^{HectPH1-}$ and in the double mutant HSB1^{acrA-}

We investigated expression of the early aggregation genes *carA* and *csaA*, encoding the cAMP receptor cAR1 and the cell adhesion molecule csA, respectively. Expression of both genes is induced at low level by starvation and strongly stimulated by cAMP pulses (Bozzaro et al., 1987a; Mann and Firtel, 1989). Consistent with a defect in ACA activation, expression of both genes is low in HSB1, with no difference between 3 and 5 h starvation time, whereas a higher expression is observed between 3 and 5 h both in AX2 and HSB1$^{HectPH1-}$ (Fig. 7A; Fig. S3B). cAMP pulsing also stimulates gene expression in HSB1, in agreement with previous results (Bozzaro et al., 1987a). Thus, inactivating HectPH1 in HSB1 appears to fully restore expression of genes required for aggregation, despite spontaneous cAMP pulsing being undetectable.

The finding that developmentally regulated cAMP-dependent genes were expressed normally in HSB1$^{HectPH1-}$ cells suggested that PKA activity was restored. PKA is the major downstream effector of adenylyl cyclase signalling inside the cell, it is required for developmental gene expression and overexpressing the PKA catalytic subunit is sufficient to induce development in ACA-null cells (Wang and Kuspa, 1997; Mann et al., 1997; Schulkes and Schaap, 1995; Williams et al., 1993). We measured PKA activity in cell extracts by assessing phosphorylation of the substrate Kemptide. As shown in Fig. 7B, cAMP stimulated PKA activity at a comparable level in aggregation-competent AX2 and HSB1$^{HectPH1-}$ cell extracts, in sharp contrast to HSB1, where PKA activity remained at vegetative levels, unless the cells were pulsed with cAMP for 5 h. Thus we conclude that, similar to with cAR1 and csA, PKA fails to accumulate in HSB1 cells that are not treated with cAMP, but accumulates normally in the double HSB1$^{HectPH1-}$ mutant.

The findings that inactivating HectPH1 in HSB1 reconstitutes development, and that exogenous cAMP pulses rescue developmental gene expression in HSB1, but in both cases without detectable activation of the adenylyl cyclase ACA, led us to study whether adenylyl cyclase B (ACB or ACR), the product of the *acrA* gene (Kim et al., 1998; Soderbom et al., 1999; Meima and Schaap, 1999), might play a role in both processes. ACB is present at a low level during aggregation and increases during the postaggregative stage, in contrast to ACA, which is maximally expressed in the pre-aggregation and aggregation stage. Inactivating the *acrA* gene results in delayed ACA accumulation, delayed cell aggregation and formation of fruiting bodies devoid of viable spores (Soderbom et al., 1999; B.P. and S.B., unpublished results).

We generated a double mutant HSB1^{acrA-} (Fig. S2D), treated the cells with cAMP pulses and checked for developmental gene expression. As depicted in Fig. 7A and Fig. S3B, *carA* and *csA* were expressed at an extremely low level in HSB1^{acrA-}, well below the level found in HSB1 cells, and cAMP pulses failed to elicit any increase in gene expression. In contrast to HSB1 cells, which displayed chemotaxis to cAMP diffusing from a microcapillary, although without forming streams, cAMP-pulsed HSB1^{acrA-} cells

Journal of Cell Science (2017) 130, 551-562 doi:10.1242/jcs.194225

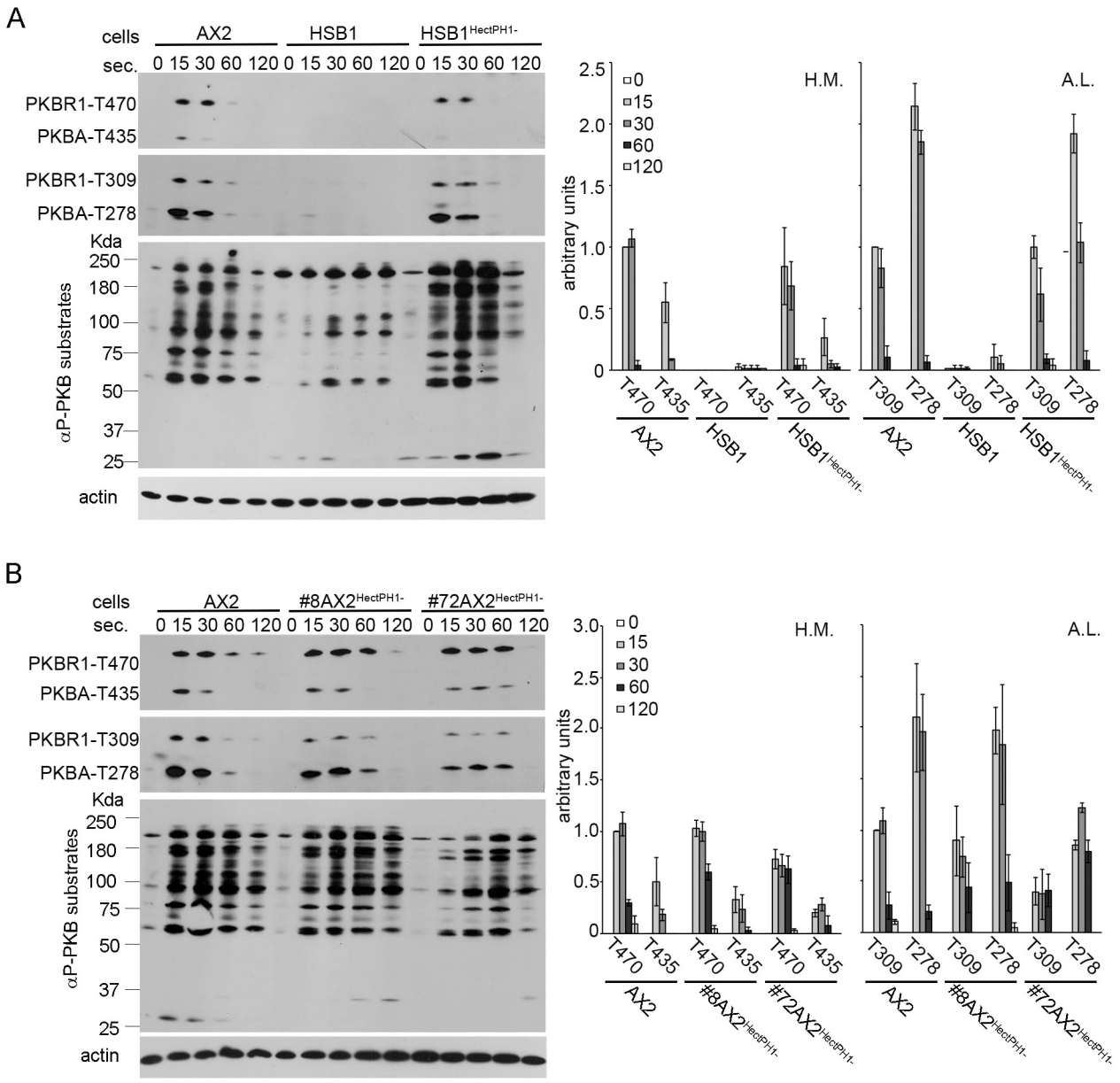

Fig. 5. PKB and PKB substrate phosphorylation in HSB1$^{HectPH1-}$ and AX2$^{HectPH1-}$ cells. (A) PKBR1 and PKBA as well as PKB substrate phosphorylation, in response to a cAMP pulse, are defective in HSB1 but restored in HSB1$^{HectPH1-}$. Cells were pulsed for 5 h with cAMP before the assay. Time 0: sample taken just before cAMP addition. T470 and T435, or T309 and T208 indicate phosphorylated HM and AL motifs, respectively, in PKBR1 and PKBA. A representative experiment is shown on the left, and normalized values of two different experiments with s.e.m. are shown in the graphs on the right. The arbitrary values were obtained by using ImageJ and first normalizing the values of phosphorylated spots for actin and then determining the ratio of each normalized value versus the AX2 value at 15 s (PKBR1-T470 or PKBR1-T309, which was set at 1). (B) PKBR1 and PKBA phosphorylation is sustained in the AX2$^{HectPH1-}$ mutant, compared to AX2. Conditions are as in A.

moved randomly, with very little if any orientation toward the cAMP source (Fig. 4A; Table S1).

We expected starving HSB1^{acrA-} cells to display very low basal ACA activity and no ACB activity. ACA or ACB enzymatic activities can be distinguished from each other due to their differential sensitivity to Mn^{2+} or Mg^{2+}, with Mn^{2+} activating ACA and Mg^{2+} preferentially ACB (Pitt et al., 1992; Meima and Schaap, 1999; Soderbom et al., 1999). Furthermore, G protein-dependent ACA stimulation can be assayed by challenging a cell lysate with the non-hydrolyzable analog GTPγS (Pitt et al., 1992). We measured adenylyl cyclase activity, and its induction with GTPγS, in HSB1^{acrA-} or control cells at different developmental times. Extracts were prepared from all cell lines at the beginning of starvation (*t*0), after cAMP pulsing for 5 h under shaking (aggregation-competent cells), or from AX2 and HSB1 at mound and pre-culminant stages (both cell strains were incubated at 13°C to allow development to proceed in HSB1 cells). As HSB1^{acrA-} cells fail to develop also at 13°C, cell extracts were prepared in parallel with the HSB1 extracts). Mn^{2+}-dependent ACA activity increased sharply in both AX2 and HSB1 cells during the first 5 h of starvation under shaking, and at the mound stage on agar, decreasing at the pre-culminant stage. In HSB1^{acrA-} cells, a 10- to 20-fold lower ACA activity was measured (Fig. 7C). When assayed in the presence of Mg^{2+}, no ACB activity was detected in HSB1^{acrA-}

Journal of Cell Science (2017) 130, 551-562 doi:10.1242/jcs.194225

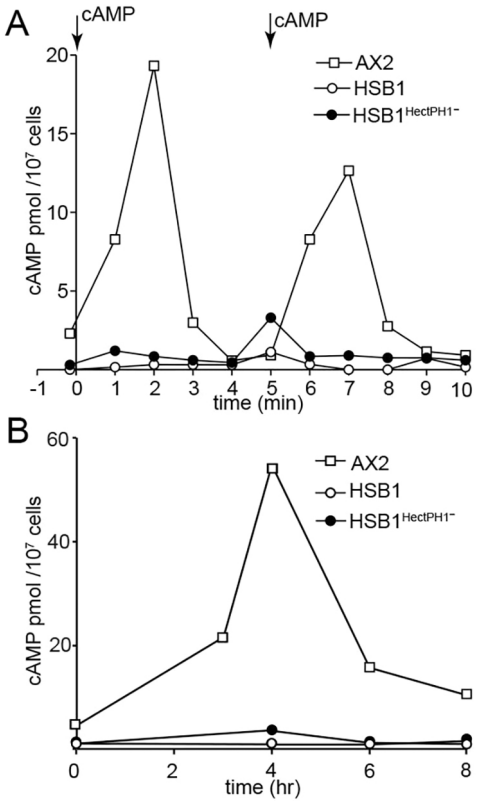

Fig. 6. cAMP fails to accumulate in HSB1 and HSB1$^{HectPH1-}$ cells. (A) Starving cells under shaking were treated with cAMP pulses every 6 min for 5 h. After 5 h, in-between two subsequent cAMP pulses (arrows), samples were withdrawn at the indicated times and cAMP assayed by radioimmunoassay. In response to a cAMP pulse, cAMP is transiently produced by AX2 cells, peaking at 2 min and decreasing thereafter. No significant increase is detectable in HSB1 and HSB1$^{HectPH1-}$ cells. A representative experiment is shown. A summary of all experiments is shown in Fig. S3A. (B) During the first 5 h of starvation, cAMP production increases in starving wild-type AX2 cells under shaking, concomitantly with aggregate formation. No detectable changes in cAMP concentration above the level found at the end of the growth phase are observed in HSB1 and HSB1$^{HectPH1-}$ cells. The experiment was repeated twice with a similar trend.

cells, as expected, whereas in AX2 and HSB1 there was a comparable steady increase from *t*0 to the pre-culminant stage (Fig. 7C). GTPγS stimulated adenylyl cyclase activity more than 10-fold in cAMP-pulsed AX2, but only minimally in HSB1 and HSB1$^{HechtPH1-}$ cell extracts, consistent with the requirement of Pia for G protein-dependent ACA stimulation. No stimulation was observed in HSB1^{acrA-} cells (Fig. 7D).

In conclusion, the parental mutant strain HSB1, although having comparable basal activities of both adenylyl cyclases ACA and ACB to that in AX2, is strongly inhibited in G protein-dependent ACA activation, consistent with the temperature-sensitive defect in Pia. In contrast, HSB1^{acrA-} fails to express ACB activity, due to ACB disruption, and displays less than 10% of the ACA activity of parental strain, even after cAMP pulsing, due to the additional defect in Pia-dependent ACA stimulation. The inability to detect GTPγS stimulation of adenylyl cyclase in these latter cells is likely due to the negligible level of basal ACA activity.

DISCUSSION

Suppression, by random mutagenesis, of a pre-existing mutation is a powerful tool for examining gene function or interactions. In this paper, we exploited REMI-mediated random insertion of blasticidin-resistance in the genome of the nitrosoguanidine aggregation-deficient mutant HSB1 to generate revertant mutants, thus identifying suppressor genes. In two clones in which development was fully restored, the same gene was disrupted, which encoded a newly discovered HECT E3 ubiquitin ligase, which had a ubiquitin ligase domain that was homologous to the HECT domain of mammalian HERC1. HERC1 belongs to the class 1 family of HECT E3 ubiquitin ligases, which also includes HERC2 and the small HERC proteins, and which usually contain a SPRY domain (Grau-Bove et al., 2013; Scheffner and Kumar, 2014). Although HECT E3 ubiquitin ligases appear to regulate many physiological processes, including membrane receptor and transporter trafficking, mTOR signalling, and transcription or chromatin remodelling, the exact function of HERC1 and HERC2 remain unclear (Sanchez-Tena et al., 2016; Rotin and Kumar, 2009; Garcia-Gonzalo and Rosa, 2005). The HECT domain of HERC1 has been shown to conjugate ubiquitin through its active site cysteine, indicating that it is very likely a functional ubiquitin ligase, but no clear substrates have been identified so far (Sanchez-Tena et al., 2016). HERC2 has been shown to regulate the stability of several proteins involved in DNA damage repair. Additionally, it targets the deubiquitinating enzyme USP33, involved in cancer cell migration, and β2-adrenergic receptor signalling (Chan et al., 2014).

Similar to mammalian HERC1 and HERC2, *Dictyostelium* HectPH1 is a giant protein with a conserved HECT domain at the C terminus, and a PH and a SPRY domain upstream, but it does not possess the RLD domains typical of HERC1 and HERC2. The isolated PH domain fused with GFP displays cytosolic distribution, enrichment in the nucleus and sometimes in the plasma membrane (Fig. S4) suggesting that HectPH1 can transitorily bind plasma membrane phosphoinositides, where it could display its ubiquitin ligase activity. Interestingly, mammalian HERC1 binds to phosphatidylinositol 4,5-bisphosphate sites via the RLD1 domain (Garcia-Gonzalo and Rosa, 2005). The SPRY domain could mediate binding of potential ubiquitylation substrates (Nishiya et al., 2011) or facilitate HectPH1 interaction with other proteins (Tae et al., 2009). The 2500-amino-acid N-terminal stretch upstream of the SPRY domain does not display any recognizable domains, but harbours several motifs that could be involved in regulation, including GSK3, PKA and Ca^{2+}/calmodulin kinase phosphorylation sites.

The HECT domain contains a conserved cysteine residue (LPEAQT**C**FFTL) that is essential for activity (Scheffner et al., 1995; Huang et al., 1999). We have shown that transfecting the HECT^{wt} domain is sufficient to abrogate the rescue of aggregation in HSB1$^{HectPH1-}$, restoring the aggregation-less HSB1 phenotype, whereas replacing the cysteine residue with serine (HECT^{C5185S}) results in an inactive HECT, when overexpressed in the suppressor background.

The HSB1$^{HectPH1-}$ mutant displays almost complete reversion of the aggregation-less HSB1 phenotype, despite the finding that Pia-dependent ACA activation was not rescued, thus confirming that Pia is still inactive in HSB1$^{HectPH1-}$ cells. Although Pia, like the other interacting subunits of the TORC2 complex, fails to form a stable complex with TOR (Cai et al., 2010), ACA activation in *Dictyostelium* appears to require a pre-formed TORC2 complex (Lee et al., 2005).

How can this complex phenotype be explained? It is worth remembering that exogenously applied cAMP pulses rescue developmentally regulated gene expression in HSB1, similar to in the *piaA*-null mutant (Chen et al., 1997), but the aggregates formed

Journal of Cell Science (2017) 130, 551-562 doi:10.1242/jcs.194225

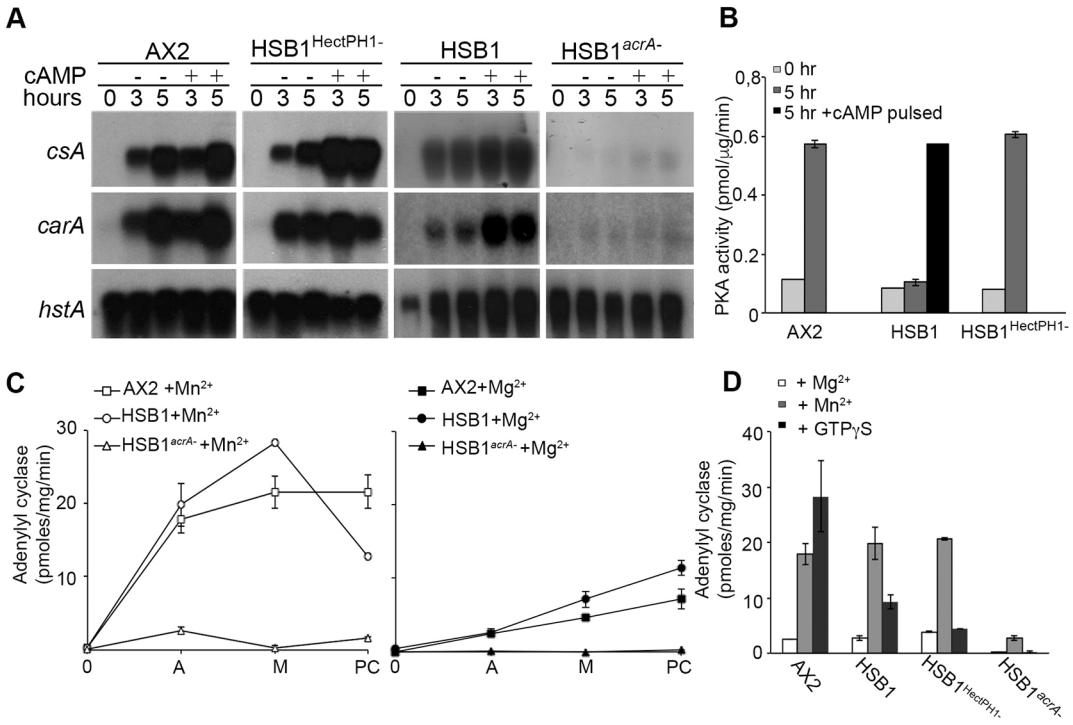

Fig. 7. cAMP-regulated gene expression and PKA activity are defective in HSB1 and restored in HSB1$^{HectPH1-}$ cells. (A) Northern blots of total RNA extracted at the indicated times from starving cells, treated or not with cAMP pulses, and labelled with *csA*, *carA* or, for normalization, *hstA*. Expression of *csA* and *carA* genes is induced by starvation and enhanced by spontaneous cAMP pulsing. Unlike AX2, in HSB1 cells, expression of both genes is reduced, with no enhancement between 3 and 5 h, consistent with the inability to activate cAMP relay. In HSB1$^{HectPH1-}$ expression of both genes is comparable to that in AX2. Exogenous cAMP pulses lead to further increase in all strains, as expected. In HSB1^{acrA-}, faint expression of both genes is observed at 3 and 5 h, with a negligible effect of cAMP pulses, suggesting that expression of ACB is essential for the increase in expression, at least if ACA is inactive. A representative experiment is shown of a total of three. For quantitative data see Fig. S3B. (B) Basal and cAMP-induced PKA activity in cell lysates. PKA activity is similar in 5-h starved AX2 and HSB1$^{HectPH1-}$, but very low in HSB1 cell lysates, although it is restored to a normal level by 5-h cAMP pulsing. This suggests that PKA fails to accumulate in HSB1 due to the impaired cAMP relay, but accumulates normally upon HectPH1 disruption. Mean±s.d. values of two experiments are shown. (C,D) ACA fails to accumulate in HSB1 in the absence of ACB. Mn^{2+} and Mg^{2+} stimulate the basal activity of ACA and ACB, respectively. ACA and ACB activities increase in AX2 and HSB1 cells under shaking at 23°C (labelled A), or at mound and pre-culminant stages (labelled M and PC, respectively), when plated on agar at 13°C. ACA activity fails to increase in HSB1^{acrA-} cells under similar conditions. (D) ACA activity is stimulated very weakly by GTPγS in HSB1 cells, due to Pia being defective, as is the case for HSB1$^{HectPH1-}$, but does not increase at all in HSB1^{acrA-} cells, presumably due to ACA failing to accumulate. Mean±s.d. values of two experiments are shown.

under shaking disaggregate once deposited on glass, and fail to proceed further in development (Bozzaro et al., 1987a). On the other hand, HSB1 cells can aggregate and form fruiting bodies on agar if mixed with 10–20% AX2 cells (Bozzaro et al., 1987a), suggesting that synergy with even a few wild-type cells acting as a autonomous, long-lasting source of cAMP is sufficient to rescue HSB1 cells, despite their inability to relay cAMP signals. This does not occur if the *acrA* gene, encoding adenylyl cyclase B, is inactivated in HSB1. HSB1^{acrA-} cells also fail to respond to exogenous cAMP pulses, in contrast to parental HSB1 cells, suggesting that ACB is essential for transducing exogenous cAMP signals, at least when G protein–ACA stimulation is impaired. This notwithstanding, there is only a negligible increase in cAMP accumulation in HSB1$^{HectPH1-}$ compared to cAMP-pulsed HSB1 cells, despite HSB1$^{HectPH1-}$ being able to aggregate and complete development.

If cAMP concentration remains at a very low level in HSB1$^{HectPH1-}$, an intriguing possibility is that disruption of the HectPH1 ubiquitin ligase could lead to hypersensitivity to cAMP signals, such that low concentrations of cAMP could activate downstream pathway(s) regulating developmental gene expression and chemotaxis, thus allowing cells to aggregate and form fruiting bodies. In favour of this hypothesis, both HSB1$^{HectPH1-}$ and AX2$^{HechPH1-}$ displayed a more efficient chemotactic index than AX2, particularly at lower cAMP concentrations. Hypersensitivity to cAMP could also explain the observed effect of HectPH1 disruption in the AX2 background, namely a delay of few hours in the beginning of aggregation and a lower efficiency of aggregation. In contrast to HSB1$^{HectPH1-}$, the AX2$^{HectPH1-}$ strain would resemble AX2 cells exposed to high concentrations of cAMP, which is known to inhibit, rather than stimulate, cAMP-dependent developmentally-regulated gene expression as well as cAMP relay (Rossier et al., 1979; Mann and Firtel, 1987; Brzostowski et al., 2013).

Hypersensitivity may occur at different levels, starting with the cAMP receptors to downstream pathways. Desensitization of the cAMP receptors could, for example, be altered in the suppressor mutant. Little is known about cAMP receptor desensitization. Upon cAMP binding, the cAR1 receptors are phosphorylated, with phosphorylation inducing loss of ligand binding (Kim et al., 1997). Inhibiting phosphorylation results in unaltered ligand binding, which leads to formation of smaller aggregates and disruption of cell streaming (Brzostowski et al., 2013), a phenotype resembling the HSB1$^{HectPH1-}$ mutant. It is possible that HectPH1 ubiquitylates the cAR1 receptors or arrestins (Cao et al., 2014), with its disruption favouring membrane exposure of the receptors, thus increasing

Journal of Cell Science (2017) 130, 551-562 doi:10.1242/jcs.194225

sensitivity to cAMP. A few E3 ligases attaching ubiquitin to specific GPCRs have been identified in other systems (Haglund and Dikic, 2012) (Alonso and Friedman, 2013; Marchese and Trejo, 2013). Persistent signal sensitivity could also result from altered receptor degradation due to impaired ubiquitylation of proteins involved in endosome-to-lysosome trafficking (Feinstein et al., 2011; Haglund and Dikic, 2012; Holleman and Marchese, 2014; Alonso and Friedman, 2013). The finding that the K_d of cAMP receptors in cAMP-binding assays is higher in HSB1$^{HectPH1-}$ may point in this direction, suggesting that two sequential events, linked to Pia and HectPH1 being both defective, are required for changing the affinity of the receptors. More experiments are required to unravel the dynamics of cAMP receptors and its regulation, and analysis of both mutants should prove to be very useful in this regard. An alternative possibility is that Pia could be a direct substrate of HectPH1, such that inactivating the ubiquitin ligase could result in increased accumulation of the protein. Overexpression of the mutated protein resulted in partial recovery of the mutant phenotype (Pergolizzi et al., 2002), thus this possibility cannot be excluded.

HectPH1 could also regulate pathways downstream of cAR1. By excluding the G protein- and Pia-dependent ACA activation, which is not rescued in the HSB1$^{HectPH1-}$ mutant, and is not essential for stimulating developmental gene expression, as it is bypassed by exogenous cAMP pulsing in HSB1 and *piaA*-null cells, the postulated increased sensitivity to cAMP signalling could depend on a pathway parallel to ACA. A potential candidate is an ACB-linked pathway to PKA or its downstream effectors regulating expression of developmental genes. The contribution of ACB in early *Dictyostelium* development is debated (Anjard et al., 2001; Pitt et al., 1992; Meima and Schaap, 1999). Our results clearly show that the HSB1 mutant, deficient in ACA activation, is able to respond to exogenous cAMP pulses inducing expression of cAMP-dependent genes. Inactivating the ACB-encoding *acrA* gene in these cells totally inhibits both chemotaxis toward cAMP and cAMP-dependent gene expression. Thus, we suggest that ACB plays a role in mediating both processes, although this role is obscured in wild-type cells by the activity of ACA, whose expression is in any case delayed in wild-type cells in which *acrA* has been deleted (Soderbom et al., 1999; B.P. and S.B., unpublished results). As depicted in Fig. 8, if HectPH1 downregulates a component of the ACB-linked pathway to PKA and gene expression, its inactivation would resemble ACA-minus cells overexpressing the PKA catalytic subunit, which are able to develop (Wang and Kuspa, 1997). PKA could phosphorylate the GATA family transcription factor GataC (Loomis, 2014), which has been recently shown to be phosphorylated also by the GSK3 ortholog GskA (Cai et al., 2014). Periodic cAMP oscillations coordinate GataC phosphorylation with its nucleo-cytoplasmic shuttling, thus modulating its transcriptional activity. Stable nuclear localization of GataC induces precocious expression of developmentally regulated genes, including *carA* and *csA* (Cai et al., 2014). Interestingly, the activity of mammalian GATA transcription factors is regulated by phosphorylation, acetylation and ubiquitylation (Nakajima et al., 2015; Kitagawa et al., 2014). Whether GataC is a potential substrate of HectPH1 is under investigation.

PKBR1, and to a lesser extent PKBA, appear to be required for chemotactic cell polarization (Meili et al., 1999; Meili et al., 2000). Phosphorylation of PKBR1 and PKBA has been shown to depend on sequential activity of TORC2 and PDK1, which phosphorylate PKB hydrophobic motifs and activation loops, respectively (Kamimura et al., 2008; Kamimura and Devreotes, 2010; Liao et al., 2010). In cAMP-pulsed HSB1 cells, similar to in the *piaA*-null mutant, PKBR1 and PKBA are not phosphorylated, in agreement with Pia–TORC2 signalling being inactive. Both are, however, phosphorylated in the HSB1$^{HectPH1-}$ suppressor mutant, leading to phosphorylation of PKB substrates. It is possible that HectPH1 inactivation in the suppressor mutant stabilizes a putative alternative kinase to TORC2, or that its inactivation results in inhibition of a phosphatase that is antagonistic to TORC2, in the assumption that TORC2 is operating in HSB1 at a basal low level (Fig. 8). It is worth remembering that PKB regulation is a complex event involving multiple Ras proteins and downstream pathways working in parallel, cooperatively and antagonistically (Meili et al., 1999; Kamimura and Devreotes, 2010; Cai et al., 2010; Liao et al., 2010; Rodriguez Pino et al., 2015). Analysis of the HSB1$^{HectPH1-}$ mutant could contribute to a better understanding of the pathways regulating PKB activity.

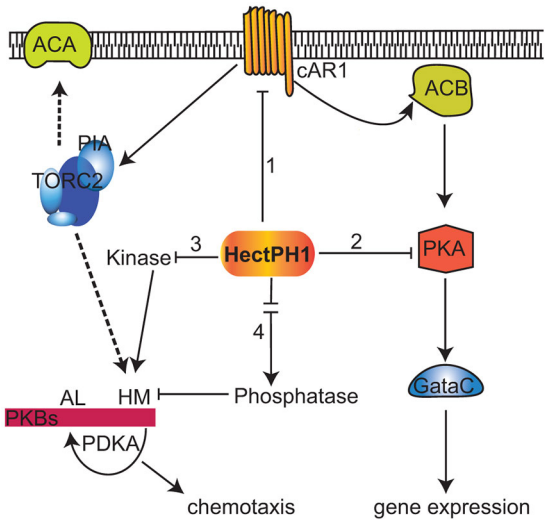

Fig. 8. Schematic model of potential HectPH1 ubiquitin targets in cAMP signalling pathways. *Dictyostelium* chemotaxis and developmentally regulated gene expression are stimulated by cAMP binding to the G protein-coupled cAMP receptor cAR1. Upon cAMP binding, cAR1 stimulates ACA, leading to production of cAMP, most of which is released and acts as chemoattractant. ACA activation requires, among other non-indicated factors, an intact TORC2 complex. TORC2 is also required for phosphorylation of PKB proteins (PKBR1 and PKBA), leading to actin recruitment and cell polarization in response to chemotactic stimuli. Owing to a mutation in the Pia subunit, TORC2 is non functional in HSB1 (dashed arrows), therefore ACA is not activated, and cells fail to secrete cAMP and to undergo cell polarization. ACB is present at low level during the first hours of starvation, accumulating in the postaggregative stages. Our data show that ACB is active in HSB1, it is also stimulated by cAR1 if cells are treated with cAMP pulses, but produces very low amounts of cAMP, which are nevertheless sufficient to stimulate developmentally regulated gene expression, very likely by activating PKA. We propose that HectPH1 could act at different levels: (1) it could directly ubiquitylate cAR1 or proteins involved in its endocytosis, therefore stimulating receptor de-sensitization and degradation; (2) it could ubiquitylate components of the PKA signalling pathway, transcription factors, such as GataC, or proteins involved in mRNA maturation, regulating developmental gene expression. In addition, we propose that HectPH1 could ubiquitylate (3) a kinase alternative to TORC2, or (4) a factor activating a phosphatase antagonistic to TORC2, thus regulating PKB phosphorylation. Inactivating HectPH1 would lead to hypersensitivity of the cells to cAMP (pathway 1 and 2) as well as PKB phosphorylation and cell polarization, even if TORC2, as in the HSB1 mutant, was totally inactive (pathway 3) or weakly active (pathway 4).

Like many HERC1 ubiquitin ligases, HectPH1 is a giant protein, but differs from large and small HERCs owing to the absence of RLD motifs and the presence of a PH domain. We have no direct evidence for ubiquitin ligase activity, but overexpressing the HECT^{wt}, in contrast to HECT^{C5185S}, domain in HSB1$^{HectPH1-}$ restored the HSB1

Journal of Cell Science (2017) 130, 551-562 doi:10.1242/jcs.194225

phenotype. It is possible that, in the absence of the long N-terminal sequence, the overexpressed HECT^{wt} domain binds E2 enzymes, transferring the ubiquitin moiety indiscriminately to specific substrates responsible for the HSB1 phenotype in addition to non-specific substrates (Weiss et al., 2010; Park et al., 2009).

It is intriguing that the HECT^{wt} domain fused with GFP is concentrated exclusively in the nucleus, both in vegetative and aggregating HSB1$^{HectPH1-}$ and AX2$^{HectPH1-}$ cells, whereas the mutated HECT^{C5185S} domain is also found in the cytosol. The fusion protein is 70 kDa in size, thus nuclear enrichment cannot be due to passive diffusion. Since the plasmid constructs do not contain nuclear localization signals typical of *Dictyostelium* (Catalano and O'Day, 2012), it is possible that the HECT domain is co-transported to the nucleus bound to a potential substrate. To what extent the nuclear localization is an artefact of the isolated HECT fragment is an open question. It is worth remembering that mammalian HERC2 is enriched in the nucleus, where it ubiquitylates several substrates. Future investigations will be directed to devising strategies to clone and express, if not the full protein, at least the entire region encompassing the SPRY, PH and HECT domains that could be used as bait to capture potential HectPH1 substrates and for biochemical and molecular genetic studies.

MATERIALS AND METHODS

Cell cultures

All strains were cultured in AX2 medium (Watts and Ashworth, 1970) at 23°C under shaking at 150 rpm in a Kuehner climoshaker (Birsfelden, Switzerland) (Bozzaro et al., 1987b). Blasticidin (InvivoGen, Toulouse, France) at 10 µg/ml final concentration was added to knockout mutants. Cells expressing GFP-fused proteins were cultured in the presence of 20 µg/ml G418 (Sigma-Aldrich, Milan, Italy). For growth on bacteria, spores or cells were mixed with *E. coli* B/2 and plated on nutrient agar plates (Bozzaro and Merkl, 1985; Bozzaro et al., 1987b).

For development, cells were washed twice in 0.017 M Soerensen Na/K-phosphate buffer, pH 6.1, resuspended at 10^7 per ml and plated on non-nutrient agar (Bozzaro et al., 1987b). For development under shaking, cells were resuspended at a concentration of 10^7 per ml in Soerensen phosphate buffer and incubated in the Kuehner climoshaker.

REMI mutagenesis, mutant suppressor screening and plasmid rescue

HSB1 cells were mutagenized by restriction enzyme-mediated insertion (REMI) of *Bam*HI-linearized pUCBsrΔBam (Adachi et al., 1994), electroporated in the presence of *Mbo*I (ThermoFisher Scientific, Waltham, MA, USA), and treated with 10 µg/ml blasticidin for 10 days (Shaulsky et al., 1996). Drug-resistant cells were plated clonally on nutrient agar in association with *E. coli* B/2. Colonies were screened visually for rescue of the HSB1 phenotype, and positive clones transferred into liquid culture for growth with blasticidin. Plasmid rescue was performed as described by Kuspa and Loomis (1992), using *Nde*I and *Eco*RV restriction enzymes for re-circularization of genomic DNA. Primers matching the *bsr*-cassette were used to sequence the genomic flanking regions, and corresponding genes were searched using the NCBI and the *Dictyostelium* database (www.dictybase.org) with the BLAST server. Protein sequence analysis was performed with the Pfam database (pfam.xfam.org). Macvector software was used for DNA sequence analysis and restriction map construction.

Generation of knockout strains

The *hephA*-knockout vector pBLS-*hephA-bsr* was constructed as depicted in Fig. S2A. After digestion with *Eco*RI and *Xba*I, the linearized DNA (10 µg) was electroporated in HSB1 or AX2 cells (Pang et al., 1999). For generating the HSB1^{acrA-} mutant, HSB1 cells were transfected with the pDG1100 plasmid (Soderbom et al., 1999). In both cases, blasticidin-resistant cells were cloned in 96-wells plates and checked for gene disruption by Southern blotting or PCR analysis (Fig. S2).

Generation of HECT^{wt}–GFP, HECT^{C5185S}–GFP, and GFP–PH (HectPH1)

The AX2 *hephA* fragment, encoding the HectPH1 HECT domain, was amplified using HD_FWD and HD_REV primers (Table S1) and cloned into the pGemT vector. A *Nco*I blunt-ended fragment was then inserted into the *gfp* 5′-end sequence in the original pDEX-H plasmid (Westphal et al., 1997), previously digested with *EcoR* I and blunt-ended, generating the plasmid pDEX-HECT^{wt}-GFP. This vector was used as template for site-directed mutagenesis. Cysteine residue 5185 in the HECT domain was mutated into a serine residue with the QuikChange II site-directed mutagenesis kit (Stratagene, La Jolla, CA), using the primers C5185S_FWD and C5185S_REV (Table S2). The resulting plasmid was named pDEX-HECT^{C5185S}GFP.

To generate GFP–PH(HectPH1), the PH-encoding fragment was amplified using PH.D_FWD and PH.D_REV primers (Table S2) and cloned into pGemT vector. A *EcoRi/ClaI* fragment was inserted into the *gfp* 3′end sequence of pDEX-H, generating the plasmid named pDEX-GFP-PH (HectPH1).

Nucleic acid analysis

Total RNA was purified using TRIzol reagent (Life Technologies, Gaithersburg, MD). RNA electrophoresis, northern and Southern blotting were performed as described previously (Bracco et al., 1997).

Chemotaxis assays

Starving cells were disaggregated by vortexing and plated onto 35-mm diameter glass-based dishes (Iwaki, Tokyo, Japan) at a density of 10^5 cell/cm^2. Chemotaxis was evaluated by local stimulation with a microcapillary (Femtotips 1, Eppendorf, Milan, Italy), filled with cAMP, using an Eppendorf micromanipulator (Peracino et al., 1998). Images were captured with intervals varying between 0.66 and 1.8 s and recorded in a Panasonic video-recorder connected to a ZVS-47DE camera, mounted on Axiovert 200 microscope (Zeiss, Oberkochen, Germany). Alternatively, images were acquired digitally with intervals of 15 s with a Lumenera Infinity 3 camera (Lumenera Corporation, Ottawa, Canada) mounted on the same microscope. Movies were analysed with ImageJ Manual Tracking and Chemotaxis/Migration plugins for determining the chemotaxis index (i.e. the directionality; the ratio between Euclidean and accumulated distance). Motility speed (accumulated distance over time) and cell polarity (ratio between length and wide) were calculated manually in at least 30 cells per movie.

The chemotaxis small population assay was performed as described previously (Kamimura et al., 2009), except that 0.8% agar containing 5 mM caffeine and Soerensen phosphate buffer were used.

cAMP binding and Scatchard analysis

cAMP binding analysis was performed as described by van Haastert (2006). Briefly, cells were incubated with 5 mM caffeine for 10 min under shaking, washed and resuspended at 10^8 cell/ml in Soerensen phosphate buffer. Aliquots of 0.08 ml were incubated with a mixture containing 0.3 mM [H^3] cAMP (Perkin Elmer, Milan, Italy), 50 mM dithiothreitol, 5 mM caffeine, and 50 to 9700 nM cAMP. After 45 s incubation at room temperature, cells were centrifuged at 14,000 ***g*** for 30 s, and the pellet was treated with 0.1 ml of 0.1 M acetic acid and dissolved in 1.3 ml scintillation fluid. Radioactivity was measured with a LS-6500 Multi-Purpose Scintillation Counter (Beckman, Indianapolis, USA). Curve fitting for cAMP saturation binding data and Scatchard plots was achieved by non-linear regression, using Prism software GraphPad (GraphPad Inc., San Diego, CA).

Biochemical assays

For cAMP-stimulated adenylyl cyclase activity, starving cells at 2×10^7 cells/ml were treated with 40 nM cAMP pulses every 6 min for 5 to 8 h. Immediately before and after a cAMP pulse, cell aliquots were collected at every minute, lysed in 3.5% perchloric acid, neutralized and assayed for total cAMP in cell lysate (Bussolino et al., 1991), using the Biotrack cAMP ^{125}I assay kit (GE Healthcare Europe, Life Sciences, Buckingamshire, UK).

The *in vitro* Mg^{2+}- or Mn^{2+}-dependent adenylyl cyclase assay was performed as described previously (Kim et al., 1998). GTPγS stimulation of adenylyl cyclase was assayed as described previously (Lilly and Devreotes, 1994; Pergolizzi et al., 2002), except that IBMX and DTT were added to inhibit cAMP phosphodiesterases.

For the PKA assay, starving cells were resuspended in 0.5 ml of cold extraction buffer (20 mM Tris-HCl pH 7.5, 4 mM $MgCl_2$, 10 mM β-mercaptoethanol, 1 µg/ml leupeptin and aprotinin) and lysed by pressing through 3 µm-pore Nucleopore filters. The lysates were clarified by centrifugation and assayed by using the SignaTECT cAMP-dependent protein kinase assay system (Promega, Madison, WI), according to the manufacturer's instructions.

PKBR1, PKBA and PKB substrate phosphorylation was assayed as described previously (Kamimura et al., 2009), after pulsing the cells with cAMP for 5 h.

Fluorescence microscopy imaging

Cells expressing GFP-fused proteins were transferred onto 36-cm^2 glass coverslips equipped with plastic rings for observation in a confocal Zeiss LSM510 microscope equipped with a 100× objective. Confocal series images were taken as described previously (Peracino et al., 2010; Buracco et al., 2015).

Acknowledgements

We thank the late W. F. Loomis for plasmid pDG1100, and A. Kamimura for helpful suggestions on PKB phosphorylation assays.

Competing interests

The authors declare no competing or financial interests.

Author contributions

B.P. and E. B. planned and conducted the experiments, collecting the data. E.B. and B.P. wrote the initial draft. S.B. conceived and supervized the study, revising the final manuscript.

Funding

This work was supported by a research grant of the Compagnia di San Paolo (12-CSP-C03-065) to S.B. and research funding of the Università degli Studi di Torino to B.P. and S.B.

Supplementary information

Supplementary information available online at
http://jcs.biologists.org/lookup/doi/10.1242/jcs.194225.supplemental

References

Adachi, H., Hasebe, T., Yoshinaga, K., Ohta, T. and Sutoh, K. (1994). Isolation of Dictyostelium discoideum cytokinesis mutants by restriction enzyme-mediated integration of the blasticidin S resistance marker. *Biochem. Biophys. Res. Commun.* **205**, 1808-1814.

Alonso, V. and Friedman, P. A. (2013). Minireview: ubiquitination-regulated G protein-coupled receptor signaling and trafficking. *Mol. Endocrinol.* **27**, 558-572.

Anjard, C., Soderbom, F. and Loomis, W. F. (2001). Requirements for the adenylyl cyclases in the development of Dictyostelium. *Development* **128**, 3649-3654.

Artemenko, Y., Lampert, T. J. and Devreotes, P. N. (2014). Moving towards a paradigm: common mechanisms of chemotactic signaling in Dictyostelium and mammalian leukocytes. *Cell. Mol. Life Sci.* **71**, 3711-3747.

Bozzaro, S. (2013). The model organism Dictyostelium discoideum. *Methods Mol. Biol.* **983**, 17-37.

Bozzaro, S. and Merkl, R. (1985). Monoclonal antibodies against Dictyostelium plasma membranes: their binding to simple sugars. *Cell Differ.* **17**, 83-94.

Bozzaro, S., Hagmann, J., Noegel, A., Westphal, M., Calautti, E. and Bogliolo, E. (1987a). Cell differentiation in the absence of intracellular and extracellular cyclic AMP pulses in Dictyostelium discoideum. *Dev. Biol.* **123**, 540-548.

Bozzaro, S., Merkl, R. and Gerisch, G. N. (1987b). Cell adhesion: its quantification, assay of the molecules involved, and selection of defective mutants in Dictyostelium and Polysphondylium. *Methods Cell Biol.* **28**, 359-385.

Bracco, E., Peracino, B., Noegel, A. A. and Bozzaro, S. (1997). Cloning and transcriptional regulation of the gene encoding the vacuolar/H+ ATPase B subunit of Dictyostelium discoideum. *FEBS Lett.* **419**, 37-40.

Brzostowski, J. A., Sawai, S., Rozov, O., Liao, X.-H., Imoto, D., Parent, C. A. and Kimmel, A. R. (2013). Phosphorylation of chemoattractant receptors regulates chemotaxis, actin reorganization and signal relay. *J. Cell Sci.* **126**, 4614-4626.

Buracco, S., Peracino, B., Cinquetti, R., Signoretto, E., Vollero, A., Imperiali, F., Castagna, M., Bossi, E. and Bozzaro, S. (2015). Dictyostelium Nramp1, which is structurally and functionally similar to mammalian DMT1 transporter, mediates phagosomal iron efflux. *J. Cell Sci.* **128**, 3304-3316.

Bussolino, F., Sordano, C., Benfenati, E. and Bozzaro, S. (1991). Dictyostelium cells produce platelet-activating factor in response to cAMP. *Eur. J. Biochem.* **196**, 609-615.

Cai, H., Das, S., Kamimura, Y., Long, Y., Parent, C. A. and Devreotes, P. N. (2010). Ras-mediated activation of the TORC2-PKB pathway is critical for chemotaxis. *J. Cell Biol.* **190**, 233-245.

Cai, H., Katoh-Kurasawa, M., Muramoto, T., Santhanam, B., Long, Y., Li, L., Ueda, M., Iglesias, P. A., Shaulsky, G. and Devreotes, P. N. (2014). Nucleocytoplasmic shuttling of a GATA transcription factor functions as a development timer. *Science* **343**, 1249531.

Cao, X., Yan, J., Shu, S., Brzostowski, J. A. and Jin, T. (2014). Arrestins function in cAR1 GPCR-mediated signaling and cAR1 internalization in the development of Dictyostelium discoideum. *Mol. Biol. Cell* **25**, 3210-3221.

Catalano, A. and O'day, D. H. (2012). Nucleoplasmic/nucleolar translocation and identification of a nuclear localization signal (NLS) in Dictyostelium BAF60a/SMARCD1 homologue Snf12. *Histochem. Cell Biol.* **138**, 515-530.

Chan, N. C., den Besten, W., Sweredoski, M. J., Hess, S., Deshaies, R. J. and Chan, D. C. (2014). Degradation of the Deubiquitinating enzyme USP33 is mediated by p97 and the ubiquitin ligase HERC2. *J. Biol. Chem.* **289**, 19789-19798.

Chen, M.-Y., Long, Y. and Devreotes, P. N. (1997). A novel cytosolic regulator, Pianissimo, is required for chemoattractant receptor and G protein-mediated activation of the 12 transmembrane domain adenylyl cyclase in Dictyostelium. *Genes Dev.* **11**, 3218-3231.

Devreotes, P. (1989). Cell-cell interactions in Dictyostelium development. *Trends Genet.* **5**, 242-245.

Dormann, D., Kim, J. Y., Devreotes, P. N. and Weijer, C. J. (2001). cAMP receptor affinity controls wave dynamics, geometry and morphogenesis in Dictyostelium. *J. Cell Sci.* **114**, 2513-2523.

Feinstein, T. N., Wehbi, V. L., Ardura, J. A., Wheeler, D. S., Ferrandon, S., Gardella, T. J. and Vilardaga, J.-P. (2011). Retromer terminates the generation of cAMP by internalized PTH receptors. *Nat. Chem. Biol.* **7**, 278-284.

Fey, P., Gaudet, P., Curk, T., Zupan, B., Just, E. M., Basu, S., Merchant, S. N., Bushmanova, Y. A., Shaulsky, G., Kibbe, W. A. et al. (2009). dictyBase–a Dictyostelium bioinformatics resource update. *Nucleic Acids Res.* **37**, D515-D519.

Garcia-Gonzalo, F. R. and Rosa, J. L. (2005). The HERC proteins: functional and evolutionary insights. *Cell. Mol. Life Sci.* **62**, 1826-1838.

Gerisch, G. (1987). Cyclic AMP and other signals controlling cell development and differentiation in Dictyostelium. *Annu. Rev. Biochem.* **56**, 853-879.

Grau-Bove, X., Sebe-Pedros, A. and Ruiz-Trillo, I. (2013). A genomic survey of HECT ubiquitin ligases in eukaryotes reveals independent expansions of the HECT system in several lineages. *Genome Biol. Evol.* **5**, 833-847.

Haglund, K. and Dikic, I. (2012). The role of ubiquitylation in receptor endocytosis and endosomal sorting. *J. Cell Sci.* **125**, 265-275.

Holleman, J. and Marchese, A. (2014). The ubiquitin ligase deltex-3l regulates endosomal sorting of the G protein-coupled receptor CXCR4. *Mol. Biol. Cell* **25**, 1892-1904.

Huang, L., Kinnucan, E., Wang, G., Beaudenon, S., Howley, P. M., Huibregtse, J. M. and Pavletich, N. P. (1999). Structure of an E6AP-UbcH7 complex: insights into ubiquitination by the E2-E3 enzyme cascade. *Science* **286**, 1321-1326.

Insall, R., Kuspa, A., Lilly, P. J., Shaulsky, G., Levin, L. R., Loomis, W. F. and Devreotes, P. (1994). CRAC, a cytosolic protein containing a pleckstrin homology domain, is required for receptor and G protein-mediated activation of adenylyl cyclase in Dictyostelium. *J. Cell Biol.* **126**, 1537-1545.

Kamimura, Y. and Devreotes, P. N. (2010). Phosphoinositide-dependent protein kinase (PDK) activity regulates phosphatidylinositol 3,4,5-trisphosphate-dependent and -independent protein kinase B activation and chemotaxis. *J. Biol. Chem.* **285**, 7938-7946.

Kamimura, Y., Xiong, Y., Iglesias, P. A., Hoeller, O., Bolourani, P. and Devreotes, P. N. (2008). PIP3-independent activation of TorC2 and PKB at the cell's leading edge mediates chemotaxis. *Curr. Biol.* **18**, 1034-1043.

Kamimura, Y., Tang, M. and Devreotes, P. (2009). Assays for chemotaxis and chemoattractant-stimulated TorC2 activation and PKB substrate phosphorylation in dictyostelium. *Methods Mol. Biol.* **571**, 255-270.

Kessin, R. H. (2001). *Dictyostelium - Evolution, Cell Biology and the Development of Multicellularity*. Cambridge, UK: Cambridge University Press.

Kim, J.-Y., Soede, R. D. M., Schaap, P., Valkema, R., Borleis, J. A., Van Haastert, P. J. M., Devreotes, P. N. and Hereld, D. (1997). Phosphorylation of chemoattractant receptors is not essential for chemotaxis or termination of G-protein-mediated responses. *J. Biol. Chem.* **272**, 27313-27318.

Kim, H.-J., Chang, W.-T., Meima, M., Gross, J. D. and Schaap, P. (1998). A novel adenylyl cyclase detected in rapidly developing mutants of Dictyostelium. *J. Biol. Chem.* **273**, 30859-30862.

Kitagawa, K., Shibata, K., Matsumoto, A., Matsumoto, M., Ohhata, T., Nakayama, K. I., Niida, H. and Kitagawa, M. (2014). Fbw7 targets GATA3

through cyclin-dependent kinase 2-dependent proteolysis and contributes to regulation of T-cell development. *Mol. Cell. Biol.* **34**, 2732-2744.
Kuspa, A. and Loomis, W. F. (1992). Tagging developmental genes in Dictyostelium by restriction enzyme-mediated integration of plasmid DNA. *Proc. Natl. Acad. Sci. USA* **89**, 8803-8807.
Lee, S., Comer, F. I., Sasaki, A., McLeod, I.-X., Duong, Y., Okumura, K., Yates, J. R., III, Parent, C. A. and Firtel, R. A. (2005). TOR complex 2 integrates cell movement during chemotaxis and signal relay in Dictyostelium. *Mol. Biol. Cell* **16**, 4572-4583.
Liao, X.-H., Buggey, J. and Kimmel, A. R. (2010). Chemotactic activation of Dictyostelium AGC-family kinases AKT and PKBR1 requires separate but coordinated functions of PDK1 and TORC2. *J. Cell Sci.* **123**, 983-992.
Lilly, P. J. and Devreotes, P. N. (1994). Identification of CRAC, a cytosolic regulator required for guanine nucleotide stimulation of adenylyl cyclase in Dictyostelium. *J. Biol. Chem.* **269**, 14123-14129.
Lim, C. J., Spiegelman, G. B. and Weeks, G. (2001). RasC is required for optimal activation of adenylyl cyclase and Akt/PKB during aggregation. *EMBO J.* **20**, 4490-4499.
Loomis, W. F. (2014). Cell signaling during development of Dictyostelium. *Dev. Biol.* **391**, 1-16.
Mann, S. K. and Firtel, R. A. (1989). Two-phase regulatory pathway controls cAMP receptor-mediated expression of early genes in Dictyostelium. *Proc. Natl. Acad. Sci. USA* **86**, 1924-1928.
Mann, S. K. and Firtel, R. A. (1987). Cyclic AMP regulation of early gene expression in Dictyostelium discoideum: mediation via the cell surface cyclic AMP receptor. *Mol. Cell. Biol.* **7**, 458-469.
Mann, S. K. O., Brown, J. M., Briscoe, C., Parent, C., Pitt, G., Devreotes, P. N. and Firtel, R. A. (1997). Role of cAMP-dependent protein kinase in controlling aggregation and postaggregative development in Dictyostelium. *Dev. Biol.* **183**, 208-221.
Marchese, A. and Trejo, J. (2013). Ubiquitin-dependent regulation of G protein-coupled receptor trafficking and signaling. *Cell Signal.* **25**, 707-716.
McCann, C. P., Kriebel, P. W., Parent, C. A. and Losert, W. (2010). Cell speed, persistence and information transmission during signal relay and collective migration. *J. Cell Sci.* **123**, 1724-1731.
Meili, R., Ellsworth, C., Lee, S., Reddy, T. B. K., Ma, H. and Firtel, R. A. (1999). Chemoattractant-mediated transient activation and membrane localization of Akt/PKB is required for efficient chemotaxis to cAMP in Dictyostelium. *EMBO J.* **18**, 2092-2105.
Meili, R., Ellsworth, C. and Firtel, R. A. (2000). A novel Akt/PKB-related kinase is essential for morphogenesis in Dictyostelium. *Curr. Biol.* **10**, 708-717.
Meima, M. E. and Schaap, P. (1999). Fingerprinting of adenylyl cyclase activities during Dictyostelium development indicates a dominant role for adenylyl cyclase B in terminal differentiation. *Dev. Biol.* **212**, 182-190.
Nakajima, T., Kitagawa, K., Ohhata, T., Sakai, S., Uchida, C., Shibata, K., Minegishi, N., Yumimoto, K., Nakayama, K. I., Masumoto, K. et al. (2015). Regulation of GATA-binding protein 2 levels via ubiquitin-dependent degradation by Fbw7: involvement of cyclin B-cyclin-dependent kinase 1-mediated phosphorylation of THR176 in GATA-binding protein 2. *J. Biol. Chem.* **290**, 10368-10381.
Nishiya, T., Matsumoto, K., Maekawa, S., Kajita, E., Horinouchi, T., Fujimuro, M., Ogasawara, K., Uehara, T. and Miwa, S. (2011). Regulation of inducible nitric-oxide synthase by the SPRY domain- and SOCS box-containing proteins. *J. Biol. Chem.* **286**, 9009-9019.
Pang, K. M., Lynes, M. A. and Knecht, D. A. (1999). Variables controlling the expression level of exogenous genes in Dictyostelium. *Plasmid* **41**, 187-197.
Park, Y., Yoon, S. K. and Yoon, J.-B. (2009). The HECT domain of TRIP12 ubiquitinates substrates of the ubiquitin fusion degradation pathway. *J. Biol. Chem.* **284**, 1540-1549.
Peracino, B., Borleis, J., Jin, T., Westphal, M., Schwartz, J.-M., Wu, L. J., Bracco, E., Gerisch, G., Devreotes, P. and Bozzaro, S. (1998). G protein beta subunit-null mutants are impaired in phagocytosis and chemotaxis due to inappropriate regulation of the actin cytoskeleton. *J. Cell Biol.* **141**, 1529-1537.
Peracino, B., Balest, A. and Bozzaro, S. (2010). Phosphoinositides differentially regulate bacterial uptake and Nramp1-induced resistance to Legionella infection in Dictyostelium. *J. Cell Sci.* **123**, 4039-4051.
Pergolizzi, B., Peracino, B., Silverman, J., Ceccarelli, A., Noegel, A., Devreotes, P. and Bozzaro, S. (2002). Temperature-sensitive inhibition of development in Dictyostelium due to a point mutation in the piaA gene. *Dev. Biol.* **251**, 18-26.
Pitt, G. S., Milona, N., Borleis, J., Lin, K. C., Reed, R. R. and Devreotes, P. N. (1992). Structurally distinct and stage-specific adenylyl cyclase genes play different roles in Dictyostelium development. *Cell* **69**, 305-315.
Rodriguez Pino, M., Castillo, B., Kim, B. and Kim, L. W. (2015). PP2A/B56 and GSK3/Ras suppress PKB activity during Dictyostelium chemotaxis. *Mol. Biol. Cell* **26**, 4347-4357.
Rossier, C., Gerisch, G., Malchow, D. and Eckstein, F. (1979). Action of a slowly hydrolysable cyclic AMP analogue on developing cells of Dictyostelium discoideum. *J. Cell Sci.* **35**, 321-338.
Rotin, D. and Kumar, S. (2009). Physiological functions of the HECT family of ubiquitin ligases. *Nat. Rev. Mol. Cell Biol.* **10**, 398-409.
Sanchez-Tena, S., Cubillos-Rojas, M., Schneider, T. and Rosa, J. L. (2016). Functional and pathological relevance of HERC family proteins: a decade later. *Cell. Mol. Life Sci.* **73**, 1955-1968.
Sasaki, A. T., Chun, C., Takeda, K. and Firtel, R. A. (2004). Localized Ras signaling at the leading edge regulates PI3K, cell polarity, and directional cell movement. *J. Cell Biol.* **167**, 505-518.
Scheffner, M. and Kumar, S. (2014). Mammalian HECT ubiquitin-protein ligases: biological and pathophysiological aspects. *Biochim. Biophys. Acta* **1843**, 61-74.
Scheffner, M., Nuber, U. and Huibregtse, J. M. (1995). Protein ubiquitination involving an E1-E2-E3 enzyme ubiquitin thioester cascade. *Nature* **373**, 81-83.
Schulkes, C. and Schaap, P. (1995). cAMP-dependent protein kinase activity is essential for preaggregative gene expression in Dictyostelium. *FEBS Lett.* **368**, 381-384.
Shaulsky, G., Escalante, R. and Loomis, W. F. (1996). Developmental signal transduction pathways uncovered by genetic suppressors. *Proc. Natl. Acad. Sci. USA* **93**, 15260-15265.
Soderbom, F., Anjard, C., Iranfar, N., Fuller, D. and Loomis, W. F. (1999). An adenylyl cyclase that functions during late development of Dictyostelium. *Development* **126**, 5463-5471.
Tae, H. S., Casarotto, M. G. and Dulhunty, A. F. (2009). Ubiquitous SPRY domains and their role in the skeletal type ryanodine receptor. *Eur. Biophys. J.* **39**, 51-59.
Van Haastert, P. J. M. (2006). Analysis of signal transduction: formation of cAMP, cGMP, and Ins(1,4,5)P3 in vivo and in vitro. *Meth. Mol. Biol.* **346**, 369-392.
Van Haastert, P. J. M. and Devreotes, P. N. (2004). Chemotaxis: signalling the way forward. *Nat. Rev. Mol. Cell Biol.* **5**, 626-634.
Wang, B. and Kuspa, A. (1997). Dictyostelium development in the absence of cAMP. *Science* **277**, 251-254.
Watts, D. J. and Ashworth, J. M. (1970). Growth of myxamoebae of the cellular slime mould Dictyostelium discoideum in axenic culture. *Biochem. J.* **119**, 171-174.
Weiss, E. R., Popova, E., Yamanaka, H., Kim, H. C., Huibregtse, J. M. and Göttlinger, H. (2010). Rescue of HIV-1 release by targeting widely divergent NEDD4-type ubiquitin ligases and isolated catalytic HECT domains to Gag. *PLoS Pathog.* **6**, e1001107.
Westphal, M., Jungbluth, A., Heidecker, M., Mühlbauer, B., Heizer, C., Schwartz, J.-M., Marriott, G. and Gerisch, G. (1997). Microfilament dynamics during cell movement and chemotaxis monitored using a GFP-actin fusion protein. *Curr. Biol.* **7**, 176-183.
Williams, J. G., Harwood, A. J., Hopper, N. A., Simon, M.-N., Bouzid, S. and Veron, M. (1993). Regulation of Dictyostelium morphogenesis by cAMP-dependent protein kinase. *Philos. Trans. R. Soc. Lond. B Biol. Sci.* **340**, 305-313.
Xiao, Z., Yao, Y. H., Long, Y. and Devreotes, P. (1999). Desensitization of G-protein-coupled receptors: agonist-induced phosphorylation of the chemoattractant receptor cAR1 lowers its intrinsic affinity for cAMP. *J. Biol. Chem.* **274**, 1440-1448.
Zhang, S., Charest, P. G. and Firtel, R. A. (2008). Spatiotemporal regulation of Ras activity provides directional sensing. *Curr. Biol.* **18**, 1587-1593.

Table S1. Chemotactic parameters of the cells shown in Fig. 4A

Cells	AX2	HSB1	HSB1$_{HectPH1-}$	HSB1$_{acrA}$
Directionality	0.73 + 0.09	0.86 + 0.43	0.77 + 0.05	0.355 + 0.03
Speed (µm/min)	15.25 +1.50	8.69 + 0.87	11.33 + 1.28	3.59 + 0.54
Polarity	6.23 + 0.53	1.66 + 0.12	3,71+ 0.30	1.65 + 0.11

The movies, from which the images in Fig. 4A were extracted, were analysed using ImageJ Manual Tracking and Chemotaxis/Migration plugins for determining the chemotaxis index, i.e. cell directionality (ratio between Euclidean and accumulated distance), cell motility speed (accumulated distance over time) and cell polarity (ratio between cellular length and wide) for at least 30 cells per movie.

Table S2. Oligonucleotide sequences of the different primers and their application.

Application	Name	Sequence
HECT Domain Amplification	HD_FWD	5'-CCATGGGTACATCATCACCAAC-3'
	HD_REV	5'-CCATGGAATTGAACGAAATCAG-3'
PH Domain Amplification	PH_FWD	5'-GAATTCTCATTTAATGAAACAACAAAAAAT-3'
	PH_REV	5'-ATCGATCAATTTCATTAATTGAAGTATTG-3'
Site Directed Mutagenesis	C5185S_FWD	5'-CTACCTGAAGCTCAAACTAGTTTCTTTACTCTCTCAATTC-3'
	C5185S_REV	5'-GAATTGAGAGAGTAAAGAAACTAGTTTGAGCTTCAGGTAG-3'
AX2$_{HectPH1-}$ Genotyping	KO_FWD	5'-GCGTTATTGCAGAAGAAGACTT-3'
	KO_REV	5'-TGATTGAATACTTGGTGTTTTCG-3'

Supplementary Movie and Figures

Movie 1. Aggregation of HSB1$_{HectPH1-}$ cells plated on agar.

Starving HSB1$_{HectPH1-}$ cells were plated on Soerensen phosphate agar at a concentration of 6.4 x 10^5 per cm2 and incubated at 22° C. After 7 hours incubation, a time lapse movie was recorded for 50 min, using Lumenera Infinity 3 camera mounted to a Zeiss Axiovert 200 microscope, with a 10x objective, with photograms taken at intervals of 15 sec.

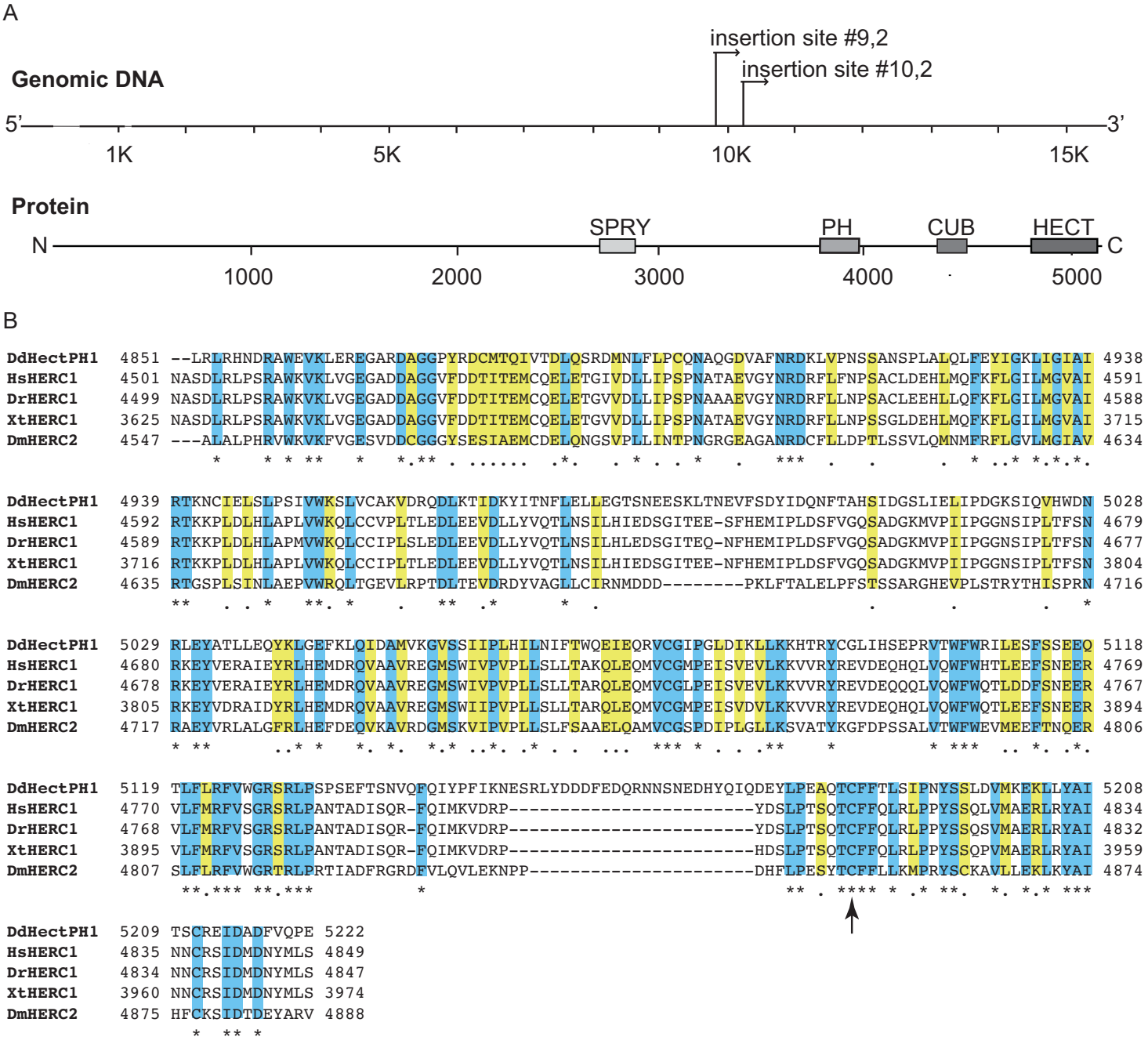

Figure S1. Diagrams of *hephA* gene and HectPH1 protein and alignment of HECT domain with close relatives.

(A) The *hephA* gene is 16053 bp in size and harbours two small introns at the 5'-end (*gray lines*). The insertion sites of the *bsr* cassette in the genomic DNA of the two suppressor mutants are indicated. The encoded protein of 5222 aa with the position of recognizable domains, in scale, is shown below.

(B) Alignment of the HECT domain of *D. discoideum* HectPH1 (DDB_G0286931), using the MacVector Clustal W program (Blosum matrix), with the closest relatives from other model organisms (*H. sapiens*, NCBI accession nr. NP_003913, *D. rerio*, NCBI accession nr XP_009301517, *X. tropicalis* NCBI accession nr. XP_012822331, *D. melanogaster*, NCBI accession nr. NP_608388). Identical aminoacid residues in all sequences are in light blue and highlighted with an asterisk, homologous residues in yellow. The arrow indicates the conservedĀcysteine residue essential for HECT activity (Scheffner et al., 1995).

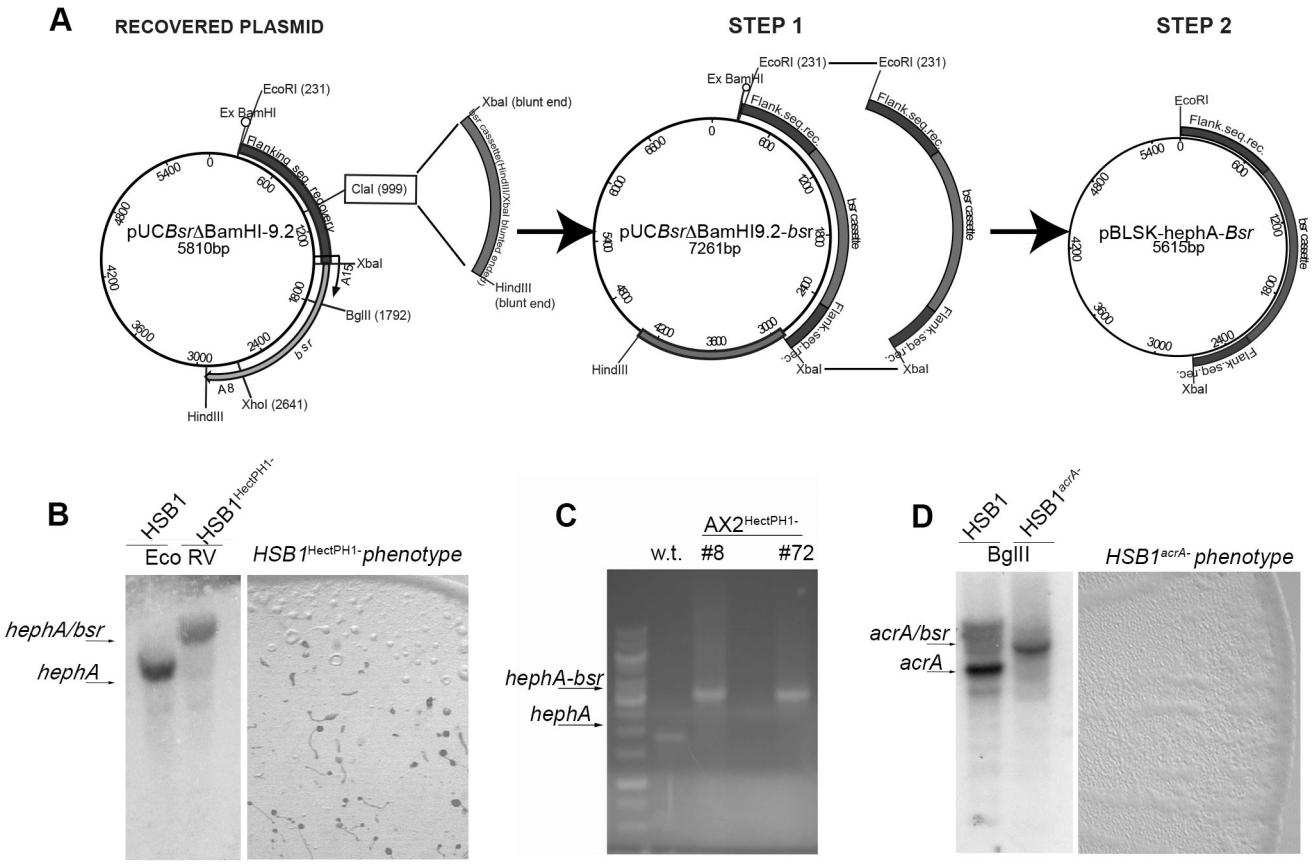

Figure S2. Construction of the plasmid pBLSK-*hephA-bsr* used for homologous recombination d genotypic d phenotypic characterization of mutants HSB1*hephA-*, HSB1*Hechtph1-* and AX2*HectPH1-*

(A) To construct the *hephA* knockout vector, the *bsr*-resistance cassette was excised from pUCBsrΔBam with *Hind*III and *Xba*I, blunt-ended with Klenow enzyme and cloned into the plasmid pUCBsrΔBam-9.2, rescued from #9.2 cells and digested previously with *Cla* I. Afterwards, the *hephA* fragment interrupted with the *bsr*-cassette was cloned into pBluescript II SK+ (Stratagene, La Jolla, CA), giving rise to the disruption vector pBLS-*hephA-bsr*. The *EcoR*I-*Xba*I fragment was used for homologous recombination.

(B and D) HSB1 was transfected with plasmid pBLSK-*hephA-bsr* or pDG1100, to obtain knockout mutants by homologous recombination in the genes *hephA* and *acrA*, respectively.

Blasticidin resistant clones were selected, DNA extracted, treated with the indicated restriction enzyme and the bands separated by electrophoresis. The Southern blots on the left shows the shift in the bands of *hephA* and *acrA* genes in two isolated clones compared to the original bands in the parental HSB1 mutant. On the right, the phenotypes of the KO-mutants are shown: HSB1^{hephA-} forms aggregates and fruiting bodies, similarly to the HSB1$^{HectPH1-}$ suppressor mutants. The HSB1^{acrA-} phenotype does not differ from the parental HSB1, in both cases a homogenous layer of non aggregating cells is visible behind the growing front.
(C) Blasticidin resistant clones from AX2 cells transfected with linearized plasmid pBLSK-*hephA-bsr* were tested by PCR for insertion of the linearized fragment in the *hephA* gene. Two positive clones, #8 and #72, that were further picked up for phenotypic characterization, are shown. W.T:Āwild type AX2 cells.

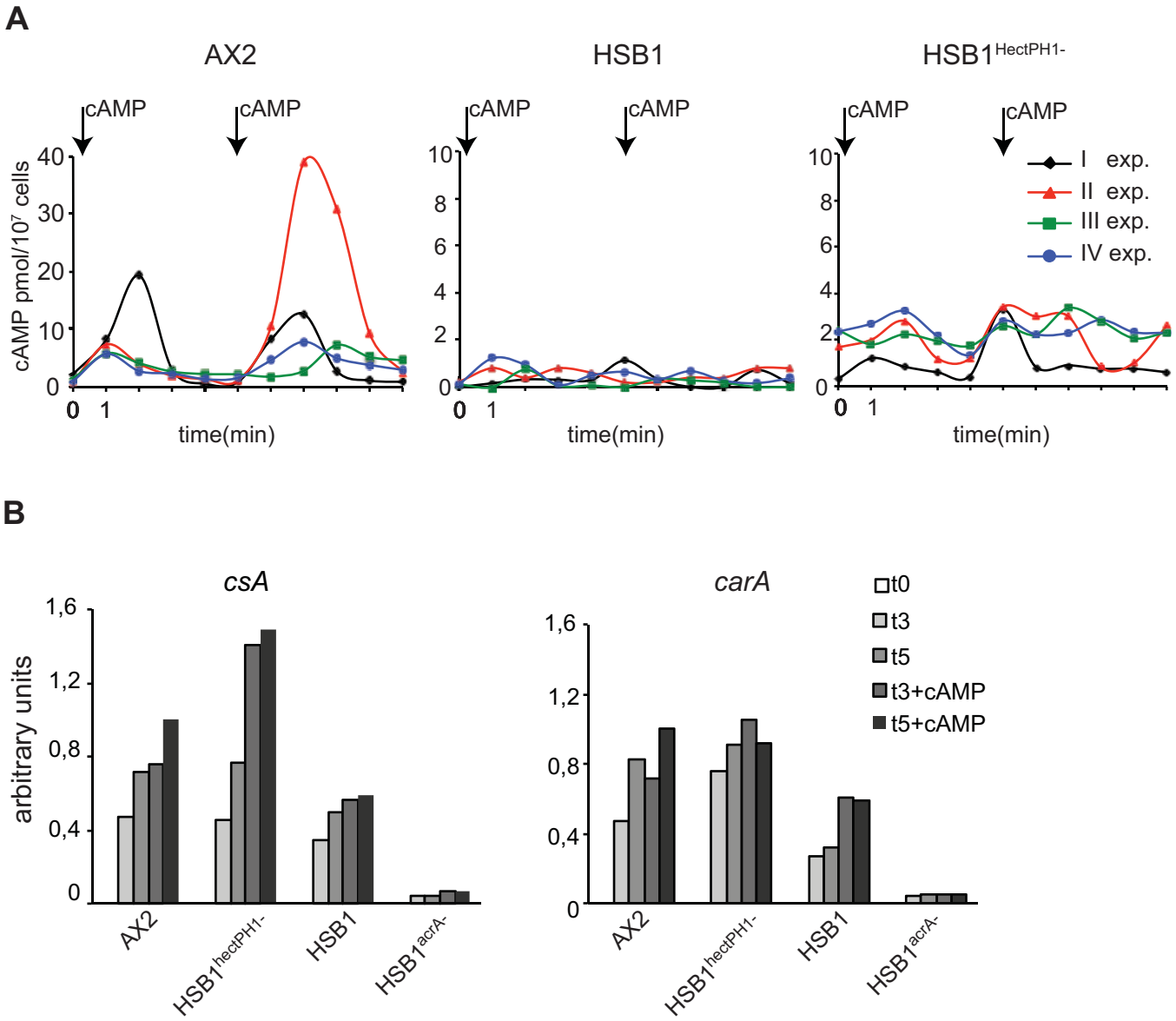

Fig. S3. cAMP accumulation in response to cAMP pulse and quantification of gene expression shown in Fig. 7A.

(A) Starving cells incubated under shaking were treated with cAMP pulses every 6 minutes for 5 hours. After 5 hours, in correspondence of two subsequent cAMP pulses *(arrows),* samples were withdrawn at the indicated times, treated with perchloric acid to inactivate enzymes, neutralized and cAMP assayed by radioimmunoassay. In response to a cAMP pulse, cAMP is transiently produced by AX2 cells, peaking at 2 minutes and decreasing thereafter. No significant increase is detectable in HSB1 and HSB1$^{HectPH1-}$ cells. Notice that the ranges in y-axis are different.

(B) The optical densities of the RNA bands shown in Fig. 7A were quantified using ImageJ , and the values normalized internally for the value of histone H1. For each gene, the normalized values shown in the abscissa for each strain were expressed as ratio to AX2 T5+cAMP.

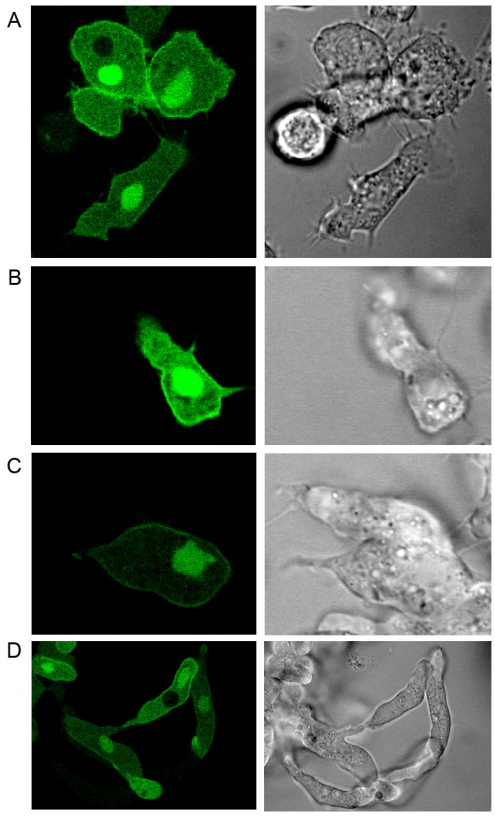

Figure S4. Cellular localization of the HectPH1 PH fragment fused to GFP.

Confocal microscopy images of living AX2 cells expressing GFP-PH(HectPH1). Green fluorescence and corresponding contrast phase are shown. *Bars*: 5 µm